GDRI GeoMech Workshop on

Advanced modelling in particulate and cohesive materials

Organized by

GDRI GeoMech & ECL-LTDS

Lyon, January 22-23 2018

GdRI GeoMech Workhsop

Lyon, 22-23 January 2018

The GDRI GeoMech international network was created in January 2016, as a follow-up of the French network GDR MeGe. During 8 years, GDR MeGe gathered the main French groups involved in the broad field of geomechanics, with a special focus on environmental applications. Taking advantage of the collaborations and connections that the partners had developed with foreign universities, extending the network in an international perspective was a natural ambition. The goal of GDRI GeoMech is thus to further promote the French community involved in geomechanics and to strengthen its national and international positioning and visibility.

Today, GDRI GeoMech brings together more than 25 partners from many countries, including the Netherlands, Italy, Spain, Canada, USA and China, with the aim of structuring the existing community working on Multi-physics and Multiscale Couplings in Geo-environmental Mechanics. Its main lines of research are:

- Catastrophic failures and triggering mechanisms
- Safety of storage reservoirs
- Energy geomechanics.

GDRI GeoMech serves as a common platform for spreading and sharing recent research outcomes, extending international collaborations as well as organizing international scientific meetings and other related events.

This booklet gathers the extended abstracts of the oral presentations given during the workshop organized at Ecole Centrale de Lyon (22-23 January 2018):

"Advanced modeling in particulate and cohesive-like materials"
Coordinators: Francesco Froiio et Eric Vincens

This topic was chosen broad enough to include or intersect most of the contributions developed in the context of the GDRI GeoMech network. During the workshop, the different approaches currently in use or being developed to model granular materials with cohesion, or cohesionless, were presented and confronted in order to highlight their differences, their commonalties, but also their own limits. Strong emphasis was given to multiple, emerging scale effects. Discrete as well as continuous techniques were discussed, with their own domains of application being put forth.

With nearly 60 attendees, coming from 3 different countries, and 20 oral presentations giving rise to extremely stimulating discussions, there is no doubt that this international workshop was a real success. The directors of the GDRI GeoMech would therefore like to express their high gratitude to Dr. Francesco Froiio and Prof. Eric Vincens, for having hosted and organized this event.

The following set of extended abstracts provides an up-to-date picture of the research activities of the GDRI GeoMech network, spanning different modelling scales, from elementary constituents (grains) to civil engineering works. This piece of work will be an excellent promoter of the GDRI GeoMech network over the forthcoming years!

This Proceeding would have never been possible without Angelika and Pierre-Yves Hicher, who have collected and revised all the abstracts. We would like to gratefully acknowledge them for their very much appreciated contribution!

Olivier Millet & François Nicot
Directors of GDRI GeoMech

The upscaling approach for granular materials:
"40 years of questions"

B. Cambou in collaboration with F. sidoroff, Ph. Dubujet, E. Vincens, H. Magoariec, C. Nouguier, S. Nguyen, …

LTDS, UMR CNRS 5513, Université de Lyon, Ecole Centrale de Lyon
Bernard.cambou@ec-lyon.fr

This presentation is not a "state of the art" but a brief synthesis of the research works developed since 1970 by B. Cambou, in collaboration with other researchers, devoted to analysing the links between local phenomena and the mechanical behaviour of granular materials at the ERV scale. Four approaches have been successively developed.

The first approach (1970 - 1975) was devoted to the **experimental analysis** of the relation between local phenomena and the mechanical behaviour of granular materials, in particular:
with J. Biarez (Grenoble): " Influence de la forme et de la dimension des particules sur les propriétés mécaniques d'un milieu pulvérulent – Influence of the form and the dimension of particles on the mechanical properties of a non-cohesive medium", First thesis Grenoble 1972
with R. Marsal (Mexico): " Etude du frottement entre matériaux rocheux – study of friction between rock materials", report Instituto de Ingenieria, UNAM, Mexico 1974.

The second approach (1975 - 1993) was devoted to the numerical analysis of the **distribution of contact forces** in a granular sample submitted to a given stress tensor. The main results can be given by the following relations:

$$\boldsymbol{f(n)} = \frac{4\pi}{3} N \overline{D} P(\boldsymbol{n}) \overline{\boldsymbol{F(n)}}$$

P(**n**): density function of contact orientations **n**. N: number of contacts per unit volume
$\overline{\boldsymbol{F(n)}}$: average value of contact forces applied on contacts sharing the contact orientation (**n**).

$$\boldsymbol{f(n)} = \mu\sigma\boldsymbol{n} + \frac{1-\mu}{2}\left[5\boldsymbol{n}\,\boldsymbol{\sigma}\,\boldsymbol{n} - tr\boldsymbol{\sigma}\right]\,\boldsymbol{n} + \mathbf{A(e)}$$

For isotropic media, term **A** is equal to zero and f(n) depends only on the contact mechanical properties characterized by parameter μ. For anisotropic media term **A** is different from zero, (Cambou & Sidoroff, 1985, Cambou & al., 1993).

The third approach (1993 – 1999) was devoted to the definition of **a change of scale in granular materials considering contacts as the micro scale** (Cambou & al 1995, Emeriault & Cambou 1996) .
Under *the kinematic localization approach* the relative displacements at contacts are approximated from the global strain tensor ($\boldsymbol{u(n)} = \boldsymbol{\varepsilon}\,\boldsymbol{l}$); then the contact forces are defined using a contact law; then an averaging operation allows the global stress tensor to be evaluated. Considering a linear elastic contact law (k^n, $k^t = \alpha k^n$), then:

$$E = \frac{3k^n(2+3\alpha)}{4\pi\,(4+\alpha)} \qquad \vartheta = \frac{1-\alpha}{4+\alpha}$$

Under *the static localization approach,* the contact forces are approximated from the global stress tensor, then the relative displacements at contacts are defined using a contact law; then an averaging operation allows the global strain tensor to be evaluated.

Local static variable: $\boldsymbol{f(n)} = \mu\boldsymbol{\sigma n} + \frac{1-\mu}{2}\left[5\boldsymbol{n}\,\boldsymbol{\sigma}\,\boldsymbol{n} - tr\boldsymbol{\sigma}\right]\,\boldsymbol{n}$ (see second approach)

For the linear elastic case: $E = \frac{30\,k^n\alpha}{2\mu^2+\alpha(10-10\mu+3\mu^2)}$ $\vartheta = \frac{2\mu^2+\alpha(5-10\mu+3\mu^2}{4\mu^2+\alpha(20-20\mu+6\mu^2)}$

The obtained results are not in good agreement with experimental or numerical (DEM) ones. It can be concluded that the kinematics at the ERV scale cannot be defined by merely considering local kinematics at contacts. It is necessary to develop another approach.

The fourth approach (2000 - 2015) was devoted to a **change of scale in granular materials considering a meso scale in 2D.**

The analysis of the kinematic variables used in the upscaling approach shows that a good agreement is obtained considering neighboring particles and not only particles in contact (Cambou & al. 2000 and 2001). Then for a 2D material, a meso-scale based on local arrays of particles (close loops of particles in contact) is considered for the upscaling approach (Nguyen & al., 2009).

Each meso-domain (Fig.1) is characterized by a loop tensor: $\boldsymbol{L}^h = \sum_1^{r^h} l^k \boldsymbol{n}^k \otimes \boldsymbol{n}^k$, two geometrical characteristics are deduced from this tensor: the orientation $\mathbf{m}^h$ which is the orientation of the major principal direction of $\mathbf{L}^h$ and the elongation ratio defined by:

$\beta^h = \sqrt{\frac{1}{2}}.\frac{L_1-L_2}{L_1+L_2}$.

For a better understanding of the local phenomena, 6 sets of meso-domains sharing common texture characteristics are considered: S1', S2', SO', W1', W2, WO. Letter S corresponds to high value of the elongation ratio, W to small values, and 1', 2', O' correspond to the compression, extension and intermediary orientations.

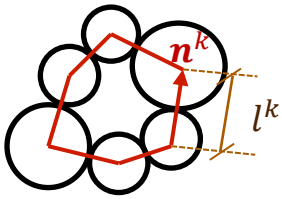

Figure 1

A tensor of anisotropy can be defined for each phase.

A **strain tensor** can be defined in the considered meso-domains. Each close loop can be partitioned into several triangles, the strain in each triangle can be easily computed from the displacements of the three vertices.

A **stress tensor** can be defined in each meso-domain from the contact forces applied on the particles defining the considered meso-domain, (Nguyen & al. 2012).

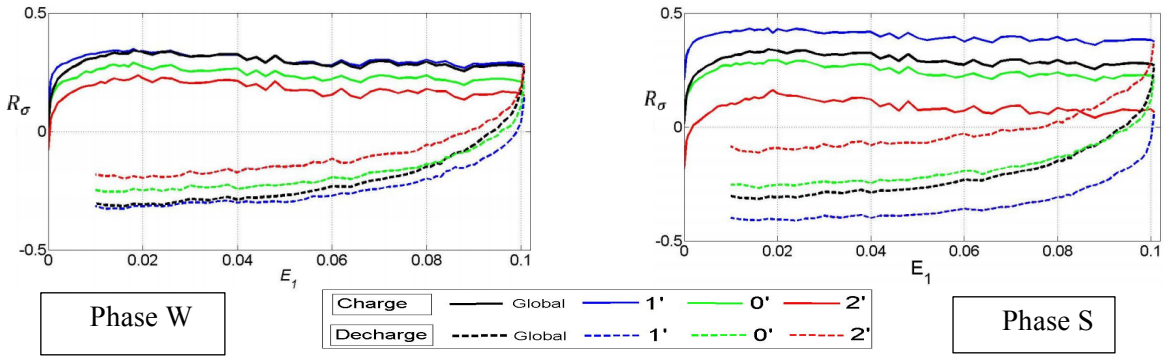

Figure 2. Behavior of the six considered phases

The analysis of the texture of the phases as well as of their behaviors shown in Figure 2 made it evident that these characteristics depend on the phase orientation with respect to the loading (1'). The volumetric average of the stresses and strains shown in Figure 2 allows the ERV stresses and strains to be computed. They show a very good agreement with the results obtained from DEM simulations which makes evident the good relevance of the variables defined at the meso-scale (texture, strains and stresses).

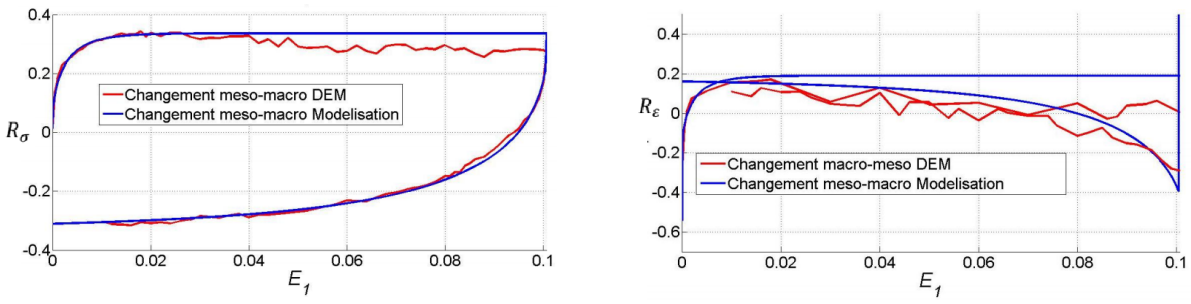

Figure 3. Comparison between DEM results and modelling using an upscaling approach (left: stress ratio, right: strain ratio).

The behavior of the six phases was modeled using a phenomenological elastic plastic model (CJS). The model parameters were evaluated considering the loading path. Different relations linking these parameters to the internal state and the phase orientations with respect to the compression direction (1') have been proposed. Using these relations made it possible to propose a forecast of the unloading path (Figure 3) in good agreement with the actual results coming from the DEM approach (Nguyen & al.,2015, Cambou & al. 2016).

An efficient constitutive law for granular materials has to take into account a good definition of the internal state. For this, the upscaling approach seems to be suitable.
The different presented analyses show the interest of considering the meso-scale in an upscaling approach for granular materials. Nevertheless, a great amount of research works is still needed to define a complete constitutive law based only on this kind of upscaling approach.

References

Cambou, B., Sidoroff F., 1985**.** Description de l'Etat d'un matériau granulaire par variables internes statiques à partir d'une approche discrète**.** *Journal de Mécanique Théorique et Appliquée*, 4 (2), pp. 223-242.
Sidoroff F., Cambou B., Mahboubi A., 1993. Contact force distribution in granular media. *Mechanics of Materials,* 16(1-2), pp. 83-89.
Cambou B., Dubujet PH., Emeriault F., Sidoroff F. 1995. Homogenization for granular materials - *European J. of Mechanics, A/Solids*, 14 (2), pp. 255-276.
Emeriault F., Cambou B., 1996. Micromechanical modelling of anisotropic non linear elasticity of granular medium. *International Journal of solids and structures*, 33(18), pp. 2591-2607.
Dedecker F., Chaze M., Dubujet P., Cambou B., 2000. Specific features of strain in granular materials. *Mechanics of cohesive frictional materials*, 5(3), pp.173-193.
Cambou,B.,Chaze M., Dedecker F., 2001. Change of scale in granular Materials . *European Journal of Mechanics A/Solids*, 19(6), pp.999-1014.
Nguyen N. S., Magoariec H., Cambou B., 2009. Analysis of structure and strain at the meso-scale in 2D granular materials. *International Journal of Solids and structures*, 46(17), pp. 3257 – 3271.
Nguyen N. S., Magoariec H., Cambou B., 2012. Local stress analysis in granular materials at a mesoscale. *International Journal of Numerical and Analytical Methods in Geomechanics*, 36(14), pp.1609-1635.

Nguyen S.K., Magoariec H., Vincens E., Cambou B., 2015. Towards a new approach for modeling the behavior of granular materials: a mesoscopic-macroscopic change of scale, *International Journal of solids and structures,* 97-98, pp. 256-274.
Cambou B., Magoariec H., Nguyen N. S., 2016. Granular Materials at Meso-scale. *ISTE press, Elsevier* 164 p.

Anisotropy and heterogeneity of internal structures in granular materials

J. Liu*,* , F. Nicot** , W. Zhou***

*State Key Laboratory of Water Resources and Hydropower Engineering Science, Wuhan University, Wuhan 430072, China
**Université Grenoble-Alpes, IRSTEA, ETNA Geomechanics Group, Grenoble 38402, France
Email: liujy@whu.edu.cn (Jiaying Liu)

Granular materials are assumed to be homogeneous at the macro scale but heterogenous at small scales. The homogeneity features has been divided by Kuhn (2003) into 5 aspects: topologic, geometric, kinematic, static and constitutive. The anisotropy of the fabric tensor is an indicator describing the topologic homogeneity.

The fabric tensor is commonly defined as the average of the contact orientations within the granular assembly:

$$\Phi_{ij} = \frac{1}{N_c} \sum_{c \in V_c} n_i n_j \tag{1}$$

where $\mathbf{n}$ is the contact normal. The second invariant of the deviatoric part of Φ_{ij} can then describe the anisotropy of the fabric tensor. Within the granular assembly, the mesoscopic grain loops (Satake, 1992) have been defined and investigated, and the fabric features of loops have been treated in previous studies, related to the analysis of the dilatancy (Kruyt and Rothenburg, 2016) and to critical state exploration (Zhu et al., 2016).

This work emphasizes the anisotropy generation within the dense and loose granular assemblies subjected to biaxial loading; and the contribution of different kinds of loops (new, lost, and constant) are investigated. In Figure 1, it can be seen that the coordination number evolutions are different for the dense and loose specimens, while the fabric anisotropy will grow for both the assemblies. Therefore the overall topology will play different roles in the anisotropy generation of these two specimens.

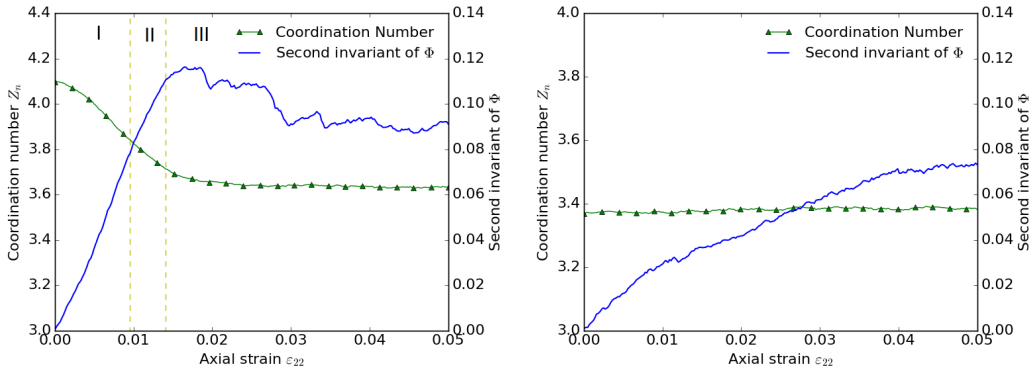

(a) (b)

Figure 1. Coordination number and fabric anisotropy of different granular assemblies: (a) dense specimen; (b) loose specimen.

In Figure 2, the average anisotropy evolutions of different kinds of loops are shown for both the dense and loose specimen. The dense granular assembly is influenced by the new and lost loops, i.e., topological changes are essential in anisotropy generation. Besides, the constant loops will also change orientation in order to adapt to the external loads. For the loose specimen, the difference between the anisotropies of new and lost loops is much smaller than for the dense one, but the total anisotropy still increases gradually. Therefore the changes in contact orientation within the constant loops should be more important.

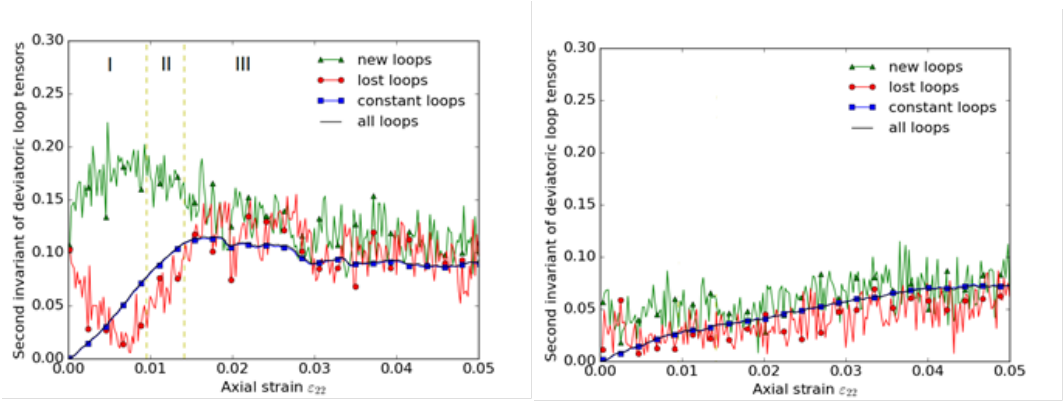

(a) (b)

Figure 2. Anisotropy generation process of new, lost and constant loops: (a) dense specimen; (b) loose specimen

The shear band will occur for the dense specimen after the stress peak. Constant loops inside and outside the shear band indicate a different anisotropy degree. The contact fabric inside the shear band will be more heterogeneous than the one outside the shear band.

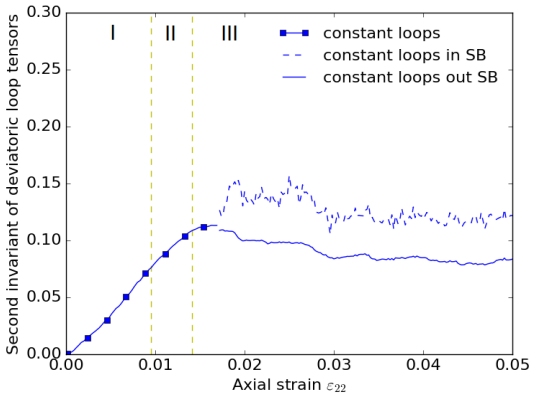

Figure 3. Anisotropy of constant loops inside and outside the shear band

In future works, the new, lost and constant loops will be investigated in terms of local dilatancy and contractancy.

References

Kruyt, N.P. and Rothenburg, L., 2016. A micromechanical study of dilatancy of granular materials. *Journal of the Mechanics and Physics of Solids*, 95, pp.411-427.

Kuhn, M.R., 2003. Heterogeneity and patterning in the quasi-static behavior of granular materials. *Granular Matter*, 4(4), pp.155-166.

Satake, M., 1992. A discrete-mechanical approach to granular materials. *International Journal of Engineering Science*, 30(10), pp.1525-1533.

Zhu, H., Nguyen, H.N., Nicot, F. and Darve, F., 2016. On a common critical state in localized and diffuse failure modes. *Journal of the Mechanics and Physics of Solids*, 95, pp.112-131.

Using DEM to model breakable grains under uniaxial compression

F. Nader* & C. Silvani* & I. Djeran-Maigre*

**INSA Lyon*
francois.nader@insa-lyon.fr

Rockfill material is increasingly used in civil engineering structures (dams, retaining walls,…) due to the multiple advantages exhibited by this material.
Grain breakage being a characteristic of this material, it is beneficial, both from an economic and a practical stand point, to develop a numerical model able to recreate the behaviour of the material, thus allowing experimental simulations.
In order to find a specific model, a polyhedral grain has been generated, and divided into tetrahedral subgrains joined together by cohesive bonds.
Single grain crushing simulations and oedometric simulations have been carried out to study the effect of multiple parameters, i.e. intra-granular cohesion and the initial grain size distribution.
The first set of simulations consists of a single grain that was crushed between two rigid plates. A series of simulations was realised for a value of the intra-granular cohesion, and a mean value of the breakage force was computed (Figure 1). An increase in the value of the cohesion joining subgrains together has shown an increase in grain strength. This result will allow modelling a specific material by choosing the cohesion that gives the material's grain strength.

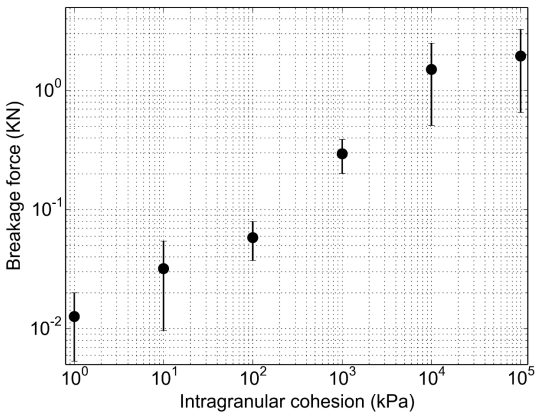

Figure 1. Variation of the breakage force of grains as a function of the intra-granular cohesion c_n - mean values and standard deviation

A second set of simulations was conducted, this time on multi-granular samples, subjected to oedometric loadings. The response of a sample of unbreakable grains was compared to that of a sample of breakable grains (Figure 2) to prove that the effect of breakage is visible, and that the sample of breakable grains is less resistant to compression, since breakage creates a greater freedom for subgrains to rearrange.

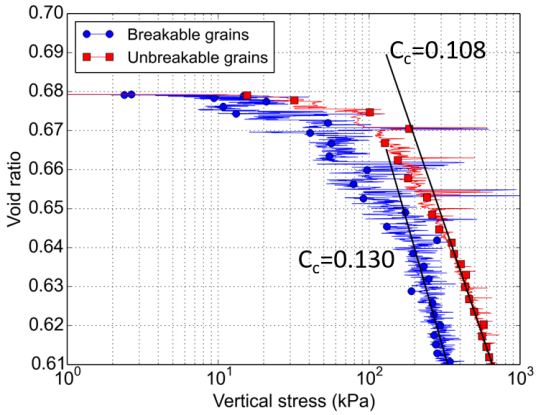

Figure 2. Oedometric curves for breakable and unbreakable grains

The effect of the intra-granular cohesion was then tested, this time on the scale of the sample. At the macroscopic scale, the effect of the cohesion cannot be clearly seen. This effect, however, is clearer at the microscopic scale when the cohesive bonds are monitored.

The last parameter to be studied was the initial grain size distribution. For this study, two samples were generated, the first with a uniform grain size distribution, the second with a graded size distribution (non uniform). The uniform grain size distribution sample had a lower initial density. Unbreakable and breakable grains were tested.

In the case of unbreakable grains, the uniform grain size distribution led to a lower resistance, which means that the sample with the higher initial density resisted compression better.

In the case of breakable grains, the opposite effect was noted: the sample with the uniform grain size distribution exhibited a higher resistance to compression. This result is in accordance with results found in the literature (Hicher & Chang, 2005) and is explained by the fact that a graded granulometry means that the smaller grains are free to move and to fill the voids between bigger grains.

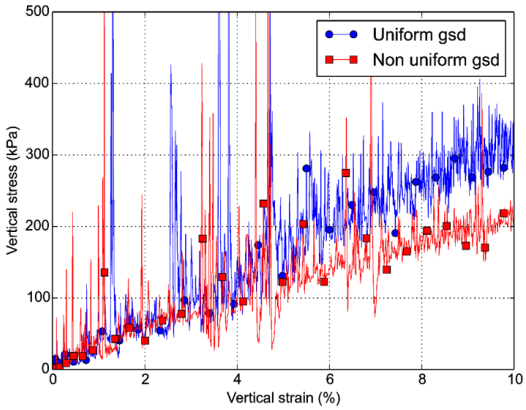

Figure 3. Vertical stress as a function of vertical strain - breakable grains - effect of the initial grain size distribution

References

Hicher, P. Y. and Chang, C. S., 2005. Evaluation of Two Homogenization Techniques for Modeling the Elastic Behavior of Granular Materials. *Journal of Engineering Mechanics*, 131(11), pp. 1184-1194.

Fabric response to strain probing in granular materials

M. Pouragha * & N.P. Kruyt ** & R.G. Wan *

**Department of Civil Engineering, University of Calgary, Canada*
*** Department of Mechanical Engineering, University of Twente, the Netherlands.*
n.p.kruyt@utwente.nl

The mechanical behaviour of jammed granular material depends heavily on the fabric of its internal contact network through which the interparticle forces transmit the stress. Contact fabric has been shown to influence many key features of granular media such as their elasticity, critical state, and dilatancy, to name a few. On the other hand, the topology of the internal contact network constantly evolves during the course of loading, rendering the knowledge of how contact fabric evolves essential for both understanding and modelling of granular materials. While the topic of fabric evolution in granular materials has been the focus of many previous micromechanical studies, such studies have been limited to only a few loading conditions such as triaxial, biaxial, or isobaric. In contrast, the current study sets out to study the evolution of contact fabric in granular materials when subjected to strain probes by performing a systematic series of Discrete Element Method (DEM) simulations. As the first study of its kind, and also due to the richness of the observed responses, the scope of the study has been limited to two-dimensional, isotropic configurations. The contributions of contact loss, gain, and reorientation mechanisms to the changes in the second-order fabric tensor have been investigated as the proportion of vertical to horizontal strain changed during a strain probing procedure. The variation of fabric evolution with strain probe direction has been shown to be captured accurately by second-order harmonic terms, as required by a representation theorem. Moreover, changes in fabric have been observed to follow a relatively linear trend with initial coordination number, which indicates a linear scaling with the number of contacts. Intriguingly, the evolution of fabric with strain probe direction shows a strong asymmetry in compression and extension, signalling an incrementally nonlinear relation between fabric and strain increments, despite the incrementally linear elastic stress-strain response. Such preliminary results suggest that the origins of the incrementally nonlinear stress-strain responses often observed in later stages of deviatoric loading of granular materials can be potentially traced back to characteristics of fabric evolution.

Quantitative prediction of discrete element models on complex loading paths

L. Sibille*, P. Villard*, F. Darve*, R. Aboul Hosn**

** Univ. Grenoble Alpes, CNRS, Grenoble INP, 3SR, F-38000 Grenoble, France.*
*** IRSTEA, Research Unit Recover, 13182 Aix-en-Provence cedex 5, France.*
Luc.sibille@3sr-grenoble.fr

The ability of the discrete element method (DEM) to describe qualitatively the constitutive behaviour of granular soils is today well established. Many works from the literature show that key features, such as the constraint of irreversible deformation by a flow rule or the non-linearity of the relation linking the incremental strain with the incremental stress, are inherent in DEM.
However, what is the ability of DEM models to produce quantitative (and not only qualitative) predictions? In the context of a civil engineering application this issue of the extent of the quantitative prediction is essential and not necessary trivial when complex loading paths, possibly non-monotonous, non-axisymmetric and with large deformations, are expected at the different points of the considered boundary value problem. Furthermore, what is the quality of such predictions with respect to those resulting from advanced phenomenological constitutive relations? In other words, is there a real advantage with respect to this point of view to implement the DEM instead of the known constitutive relations which have been validated for decades in international benchmarks?

The objective of this communication is to assess the extent of the quantitative prediction of two DEM models in terms of the mechanical response to complex loading paths (see Sibille et al., 2018 for a complete description). In order to describe realistic shear strengths, one of the models consists of spherical particles with the introduction of a rolling resistance at the inter-particle contact in addition to the Coulombian friction (Aboul Hosn et al., 2017). The other model includes clusters of spherical particles with only a Coulombian friction at the contact (Salot et al., 2009). These are relatively light DEM models involving five and four mechanical parameters, respectively. DEM predictions are evaluated by a comparison with experimental data and an advanced constitutive relation, with respect to three kinds of loading paths, all fully three dimensional in the space of principal stresses (i.e. non-axisymmetric): (i) monotonous stress proportional loading paths at a constant intermediate stress, (ii) cyclic stress proportional loading paths at a constant mean pressure (see Figure 1), and (iii) circular loading paths in the deviatoric stress plane so that the Lode angle is continuously changing while both the mean pressure and the stress deviator are constant.
The experimental responses to these loading paths result from tests performed with a true triaxial apparatus (TTA) on the Hostun sand “RF” (Lanier & Zitouni, 1988; Zitouni). Some of these tests were used as validation cases for the benchmark on constitutive relations organized for the International Workshop of Cleveland in 1987 (Saada & Bianchini, 1988). The phenomenological constitutive relation considered is an incrementally non-linear relation of second order (INL2) developed by Darve and Dendani (1988). This model includes around 20 constitutive parameters and was also used for the Cleveland workshop among the 27 constitutive relations compared for this occasion.

The framework described above leads to putting the DEM models into perspective with respect to conventional constitutive relations by taking into account the number of mechanical parameters introduced and the set of experimental data necessary for their calibration.

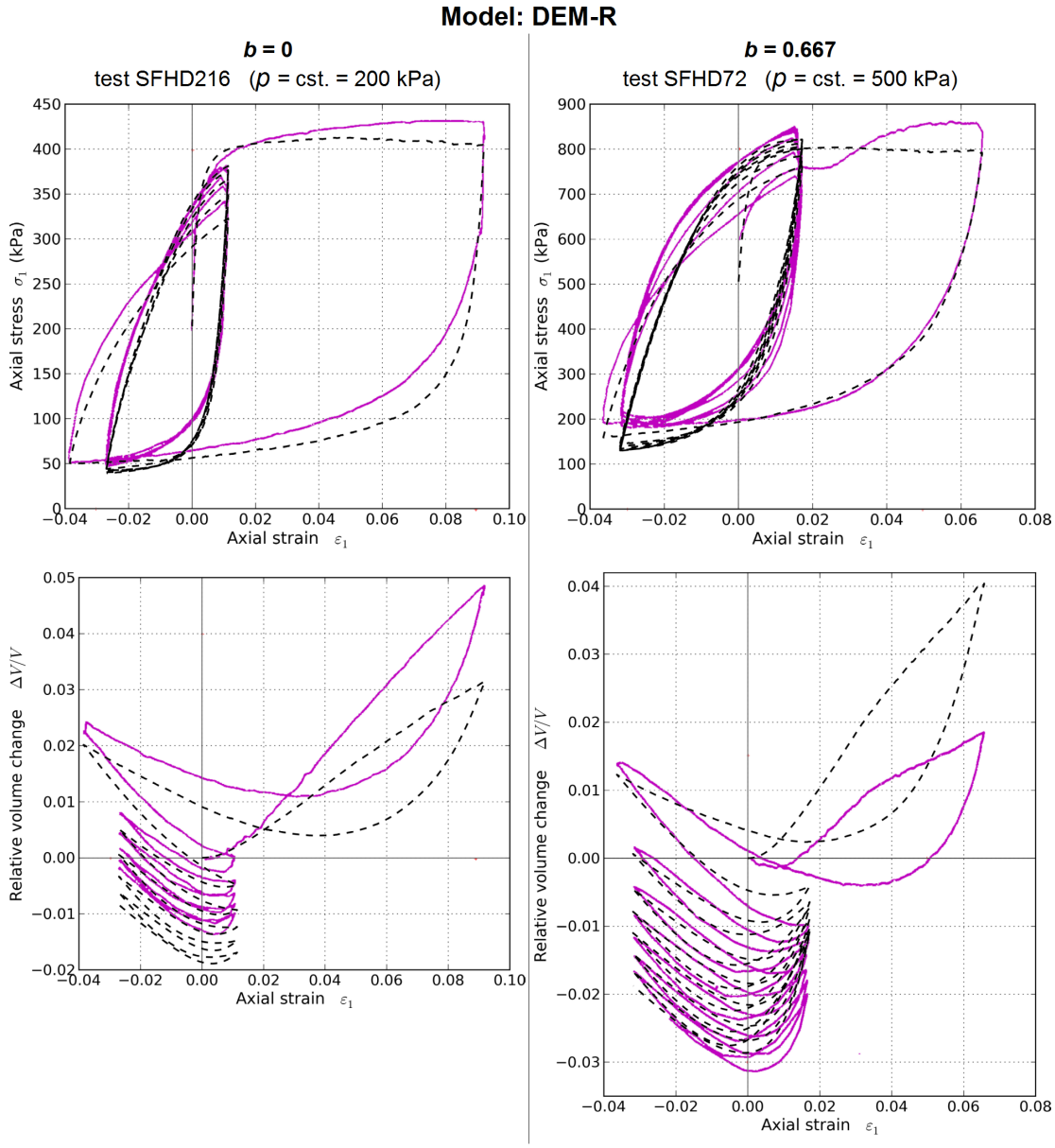

Figure 1. Comparison of experimental response (in continuous magenta line) of a dense Hostun sand sample to cyclic stress proportional loading paths at constant mean pressure with simulated responses (in dashed black line) with a discrete numerical model embedding an inter-particle rolling resistance. The b parameter, kept constant for a given loading path, is defined as $b = (\sigma_2 - \sigma_3) / (\sigma_1 - \sigma_3)$.

References

Aboul Hosn R., Sibille L., Benahmed N., Chareyre B. (2017). Discrete numerical modeling of loose soil with spherical particles and interparticle rolling friction. *Granular Matter*, 19:4. doi:10.1007/s10035-016-0687-0

Darve F. and Dendani H. (1988). An incrementally non-linear constitutive relation and its predictions. *Constitutive Equations for granular non-cohesive soils*, Cleveland ed. A.S. Saada & Bianchini, Balkema, Rotterdam: 237-254.

Lanier J. and Zitouni Z. (1988). Development of a data base using the grenoble true triaxial apparatus. *Constitutive Equations for granular non-cohesive soils*, Cleveland ed. A.S. Saada & Bianchini, Balkema, Rotterdam: 47-58.

Saada A.S. and Bianchini G. (1988). Constitutive equations for granular non-cohesive soils - *Proceedings of the international workshop on constitutive equations for granular non-cohesive soils*, 22-24 July 1987, Cleveland. Balkema, Rotterdam.

Salot C., Gotteland P., Villard P. (2009). Influence of relative density on granular materials behavior: DEM simulations of triaxial tests. *Granular Matter*, 11(4):221-236. doi:10.1007/s10035-009-0138-2.

Sibille L., Villard P., Darve F., Aboul Hosn R. (2018). Quantitative prediction of discrete element models on complex loading paths. Submitted to *International Journal for Numerical and Analytical Methods in Geomechanics.*

Zitouni Z. (1988). Comportement tridimensionnel des sables. *PhD thesis*, Université Joseph Fourier – Grenoble, France.

Multiscale modelling of partially saturated media

B. Chareyre*, C. Yuan*, E.P. Montella*,, S. Salager*, A. Gens****

**Univ. Grenoble-Alpes, Grenoble INP, 3SR lab., Grenoble, France*
*** Technical University of Catalonia (UPC), 08034, Barcelona, Spain*
bruno.chareyre@3sr-grenoble.fr

Simulating complex hydro-mechanical couplings in grain-fluid systems is a great challenge for the discrete element methods (DEM). For materials saturated by only one pore fluid, the discretization of the pore space as a network of connected pores makes it possible to simulate relatively large problems (say, thousands of solid particles at least) in three dimensions (Chareyre et al. 2012). With such a *pore-scale* approach, the dominant viscous terms can be captured without actually solving a Navier-Stokes problem (Marzougui et al. 2015). The computational cost is thus reduced by orders of magnitudes, which leads the way to more realistic simulations. A question discussed hereafter is whether this approach can be extended to account for two immiscible pore fluids in partially saturated materials?

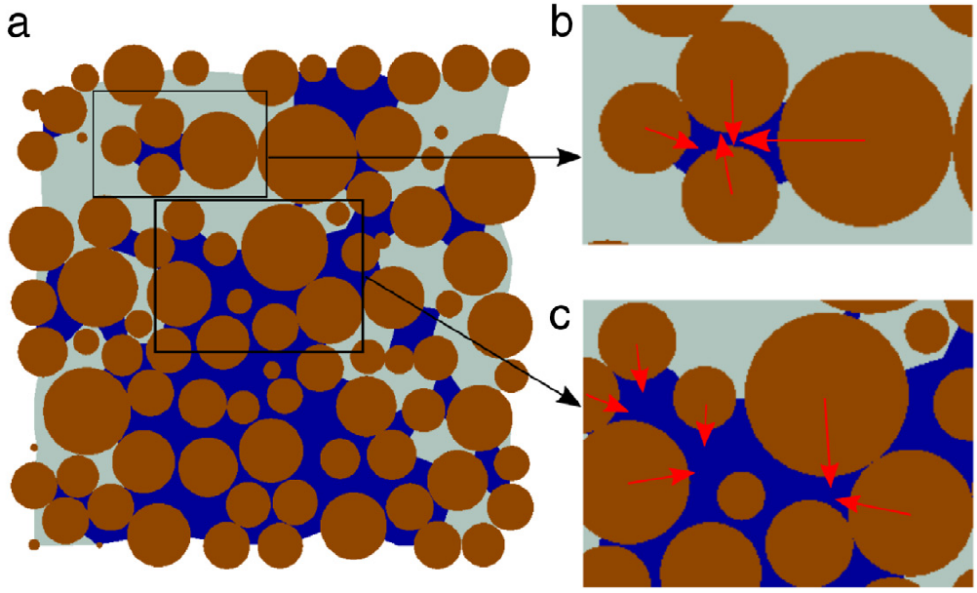

Figure 1 (a) Distribution of the wetting phase (dark blue) and the non-wetting phase (light blue) during the primary drainage of a 3D sphere packing, simulated with the pore-scale model of Yuan and Chareyre (2017); (b,c) the red arrows indicate the capillary forces on individual particles.

DEM modelling of partial saturation is not a new topic, yet the majority of previous studies have not gone beyond the so-called “pendular” regime, in which the wetting phase is present in such a little amount that it only forms pendular bridges associated to pairs of particles. In the other saturation regimes one can hardly avoid time consuming surface minimization techniques or even the direct resolution of a 2-phase fluid dynamics problem at the microscale to capture the geometry of phases and interfaces. The pore-scale approach of this problem aims to decrease significantly the computational cost. For this purpose, the movements of the fluid phases and the fluid-solid interactions are described by introducing relevant geometrical objects in a tetrahedral-based partition of the pore space together with evolution laws for

those pore-scale objects. For a range of micro-scale processes, this approach has proved to be successful and, for instance, the primary drainage of a saturated sample can be reproduced accurately (Yuan et al. 2016). Unfortunately, a number of processes still remain which demand significant improvements from both phenomenological and algorithmic points of view, such as bubble entrapment, coalescence of wetting phases, or viscous effects leading to mixed conditions of drainage-imbibition at the meso-scale.

A hybrid framework is possible to develop in which the pore-scale objects and their evolution are predicted by direct simulations through the Lattice-Boltzman method (LBM – see Montella et al. (2018)). Domain decomposition applied to a large granular specimen permits identifying relevant elementary units of the micro-structure made of less than a dozen particles typically. The LBM responses of these elementary units under particular boundary conditions are used to define a system of equations relevant to a pore-scale description of the two-phase flow problem. This numerical framework is evolutionary in the sense that the results obtained may help replace progressively LBM by analytical relationships so as to link local geometry to hydrostatic properties (e.g. entry capillary pressure of a pore throat). Ultimately, the LBM calculations may be skipped completely.

References

Chareyre, B., Cortis, A., Catalano, E., & Barthélemy, E. (2012). Pore-scale modeling of viscous flow and induced forces in dense sphere packings. *Transport in porous media*, 94(2), 595-615.

Marzougui, D., Chareyre, B., & Chauchat, J. (2015). Microscopic origins of shear stress in dense fluid–grain mixtures. *Granular Matter*, 17(3), 297-309.

Montella, E.P., Chareyre, B., Salager, S., & Gens, A. (2018) Micromechanical study of multiphase flow based on the lattice Boltzmann method, *2nd Yade Workshop*.

Yuan, C., Chareyre, B., & Darve, F. (2016). Pore-scale simulations of drainage in granular materials: finite size effects and the representative elementary volume. *Advances in Water Resources*, 95, 109-124.

Yuan, C., & Chareyre, B. (2017). A pore-scale method for hydromechanical coupling in deformable granular media. *Computer Methods in Applied Mechanics and Engineering*, 318, 1066-1079.

Suffusion micromechanics: Accounting for fluid/grains interactions

A. Wautier[1,2,3], S. Bonelli[2] & F. Nicot[3]

[1]AgroParisTech-ENGREF, 19 avenue du Maine, 75732 Paris, France.
[2] Irstea UR RECOVER, 3275 Rte Cézanne, CS 40061, 13182 Aix-en-Provence Cedex 5, France.
[3]Université Grenoble Alpes, Irstea, UR ETGR, 2 rue de la Papeterie BP 76, F-38402 St-Martin-d'Hères, France.
antoine.wautier@irstea.fr

Under various circumstances, granular materials subjected to an internal flow can undergo a selective erosion of their finest particles. When applied to dikes or dams, this phenomenon is referred to as suffusion and may lead to a loss of mechanical stability which may cause the failure of the hydraulic structure.
So far, the occurrence of suffusion has mostly been considered as the non-ability of a granular material to self-prevent the loss of the smallest particles. Such materials are said to be internally unstable (Kenney & Lau, 1985). This definition of stability is however too restrictive and the notion of mechanical stability inherited from Hill (Hill, 1958) has been preferred in this study. Hill's definition relies on the non-vanishing of the second order work, which defines a bifurcation domain formed by the set of stress states in which a suitable incremental loading can result in the effective failure of the material (Nicot et al., 2009).
While considering a granular material in an unstable state, we have recently shown that the free particles play an important role with respect to the mechanical stability by preventing large plastic strain development (Wautier, 2017). As a result, a first fluid impact on the mechanical stability of a granular material may result from the transport of these rattlers. However, a second fluid impact exists as additional forces are applied to the primary skeleton of the granular material. These additional forces lead to stress redistribution and possibly to grain detachment. In this study, we consider a representative elementary volume of a granular material prepared in an unstable stress state and deprived of its rattlers (*i.e.,* particles not in contact with any other particle). By accounting for the local fluid/grain interactions in three dimensions thanks to a DEM-PFV coupling scheme (Chareyre, 2012), the ability of a fluid flow to trigger off the underlying instability is shown. Besides, a particular attention has been paid to the flow impact on the granular force chains constituting the main loadbearing mesostructures in granular materials.

I. DEM/PFV simulations on unstable granular materials deprived from rattlers

Thanks to the use of the YADE software, a cubic assembly of 10,000 spherical particles has been generated following a uniformly distributed particle size distribution with $r_{\max} = 3.5\, r_{\min}$. At the microscale, the interactions between grains can be modeled through a classical elasto-frictional contact law with the parameters given in the Table below.

Parameters	Value
Density	3,000 kg.m-3
Young Modulus (E)	356 MPa
Stiffness ratio (ν)	0.42
Inter-particle friction angle (φ)	35°
Particle-wall friction angle	0°
Number of particles	10,000

A loose sample with a void ratio of 0.73 has been prepared and subjected to a drained triaxial under a confining pressure of 100 kPa up to a stress ratio $\eta = q/p = 0.35$. It has then been

deprived of its rattlers. For this mechanical stress state, a directional analysis performed in Rendulic's plane (Wautier, 2017) demonstrates that this sample is at a bifurcation point characterized by the existence of loading directions resulting in the vanishing of the second order work.

This numerical sample is then subjected to a macroscopic pressure gradient corresponding to a hydraulic gradient $I = 0.1$ while keeping constant the mechanical loading obtained during the triaxial loading. Two flow directions are considered as illustrated in Figure 1: parallel to the principal loading direction (vertical flow case) and perpendicular to the principal loading direction (horizontal flow case).

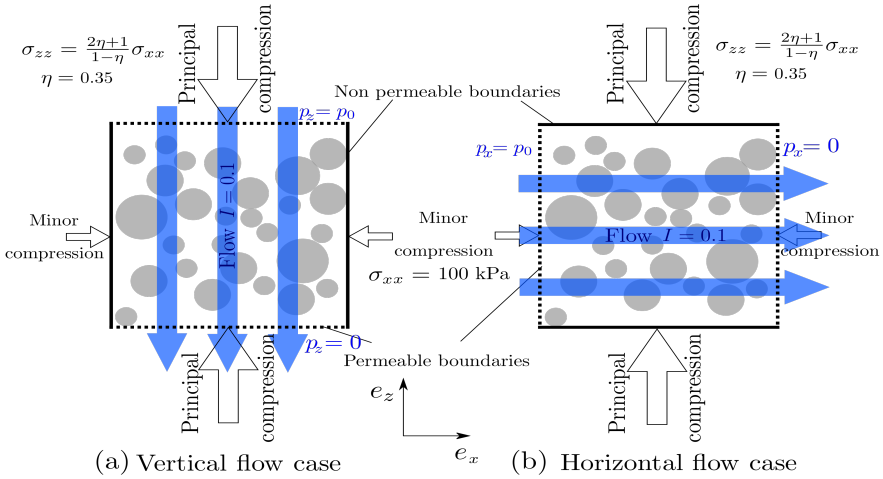

Figure 2: Boundary value problems solved.

As shown by the strain jumps observed during the time evolution of the incremental strain components plotted Figure 2, both flow cases lead to the collapse of the granular sample.

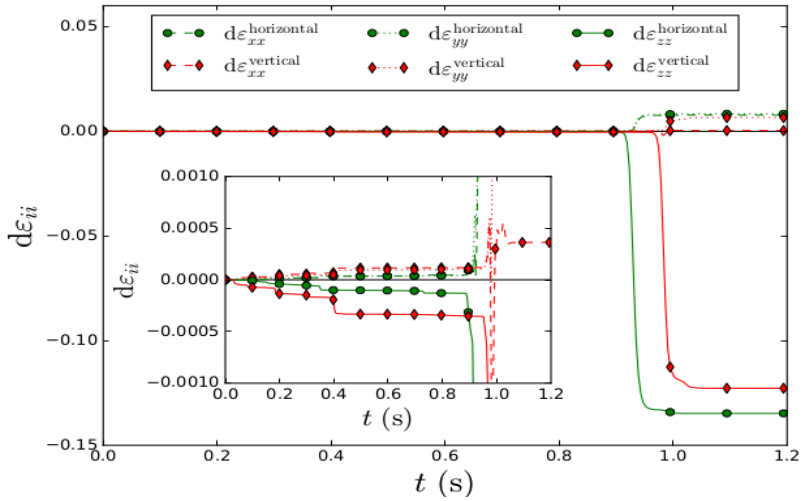

Figure 3: Incremental strain response with respect to time for the two flow cases.

II. Pressure distributions and fluid forces fluctuations

The micro perturbations induced by the fluid on the primary skeleton can be assessed by plotting the statistical distributions of the three components F_x^f, F_y^f and F_z^f of the fluid forces for the two flow cases at the beginning of the flow simulation. The corresponding probability functions (pdfs) are shown in Figure 3.

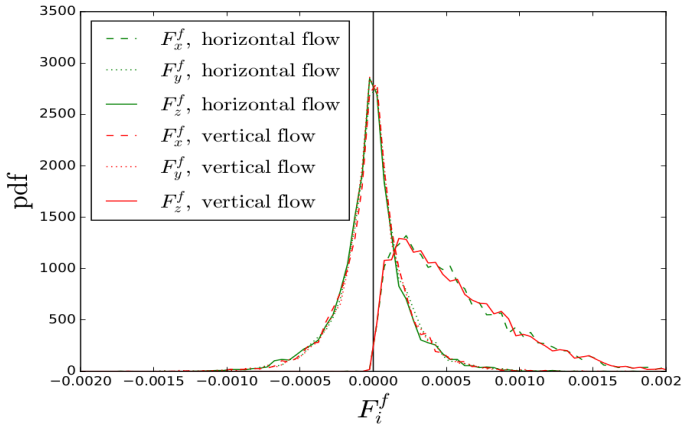

Figure 4: Pdfs for the fluid force components for the two flow cases.

The comparison between the pdfs in Figure 3 gives important clues to understand why the fluid flow direction does not influence the occurrence of macroscopic failure. Despite showing a zero mean value, the pdfs of fluid forces perpendicular to the flow direction shows a standard deviation which is non negligible compared to the pdf mode of the component along the macroscopic flow direction. As a result, local fluid force fluctuations can explain why the flow direction may not influence the triggering of the underlying instability.

As soon as the global collapse occurs, it is interesting to have a look at the pressure distribution in the pore network. For the sake of visualization, the mean $\bar{p}$ and standard deviation of the pressure field are computed on planes perpendicular to the macroscopic flow direction for varying positions between the upstream and downstream walls. In Figure 4, the difference between the actual pressure and the linear localization of the macroscopic gradient p_{th} are shown before and after the sample collapse in the vertical flow case.

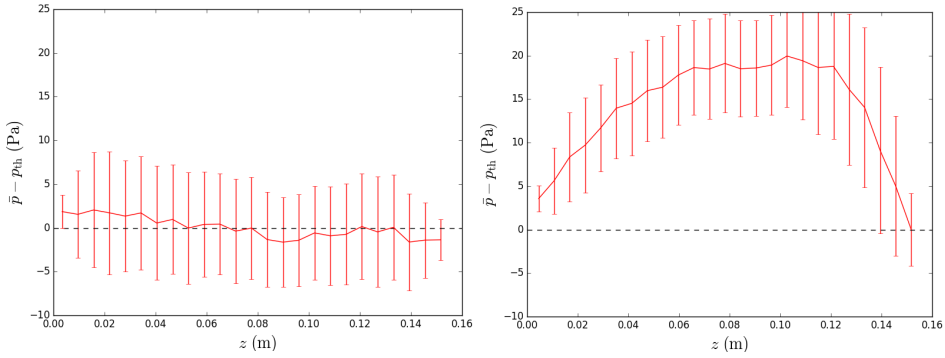

Figure 5: Difference between the mean pressure $\bar{\mathbf{p}}$ and the macroscopic linear localization $\mathbf{p_{th}}$ before (left) and during (right) sample collapse for the vertical flow case. Standard deviation are shown with error bars.

This Figure shows that the collapse is associated with an increase in the pore pressure in the core of the sample. However, this increase is a consequence of the collapse and not the cause. The collapse is thus the result from a force chain collapse and not from liquefaction.

III. Micromechanical inspection of loss of sustainability

While performing a similar micromechanical analysis of the collapse as in Wautier et al. (2018), the local failure mechanisms can be explored. By looking at the kinetic energy of the particles, it appears that outbursts of kinetic energy are a signature of the collapse. However, it is noticed that some generalised outbursts don't precede the collapse. By computing the sliding index $I_p = \frac{F_t/F_n}{\tan\phi}$ of each contact, it is possible to estimate how many contacts are close to the Mohr-Coulomb sliding limit by looking at the time evolution of the number of contacts

with $I_p > 0.9$. In Figure 5, $N(I_p > 0.9)$ is plotted for the two flow case just before the collapse. Two vertical solid lines mark the occurrence of outbursts of kinetic energy.

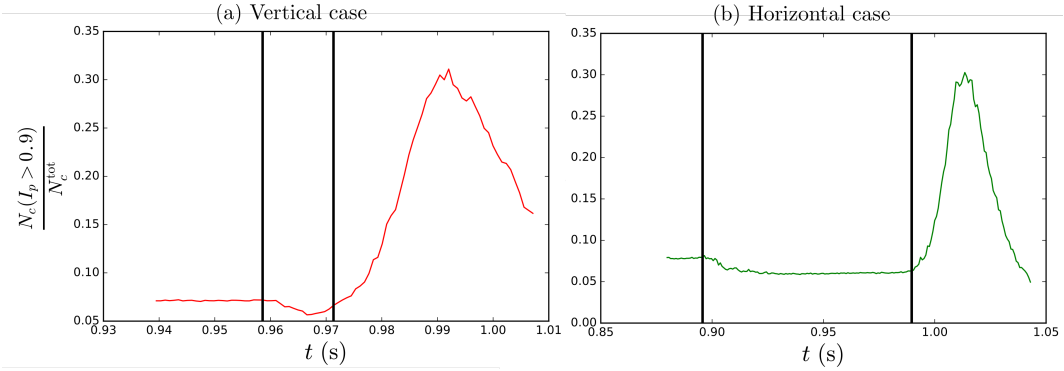

Figure 6: Time evolution of the number of contacts close to sliding for the two flow cases. Outbursts or kinetic energy are shown with vertical solid lines. The second one correspond to effective failure

While the first outburst is associated with a decrease in the contacts close to sliding, the second one is associated with an increasing number of contacts getting close to sliding.
While looking at the evolution of the force chain number and analysing the causes for the disappearing of force chains, it is noticed that the force chain bending and the stress redistribution are the main mechanisms responsible for the onset of the collapse. The effective failure of force chains occurs only later on.

Conclusion

In this study, the specific impact of a fluid flow on the primary fabric of a granular material was investigated in terms of mechanical stability thanks to DEM/PFV simulations. It was found that an internal fluid flow is able to trigger off the underlying instability without any change in the macroscopic stress state and that the flow direction has no influence because of local fluid force fluctuations. In addition, by analysing the microscale mechanisms occurring during the sample collapse, it was found that the fluid perturbation induces a decrease in kinematic constraints around the force chains which is characteristic of a local loss of stability.

References

Kenney, T., Lau, D., 1985. Internal stability of granular filters. *Canadian Geotechnical Journal* 22 (2), 215–225.

Chareyre, B., Cortis, A., Catalano, E., Barthélemy, E., 2012. Pore-scale modeling of viscous flow and induced forces in dense sphere packings. *Transport in porous media* 94 (2), 595–615.

Hill, R., 1958. A general theory of uniqueness and stability in elastic-plastic solids. *Journal of the Mechanics and Physics of Solids* 6 (3), 236–249.

Nicot, F., Sibille, L., Darve, F., 2009. Bifurcation in granular materials: An attempt for a unified framework. *International Journal of Solids and Structures* 46 (22), 3938–3947.

Wautier, A., Bonelli, S., Nicot, F., 2017. Mechanical stability of granular materials subjected to suffusion. *Extended abstracts of the GDRI meeting in Nantes 2017*

Wautier, A., Bonelli, S., Nicot, F., 2018. Micro-inertia origin of instabilities in granular materials. *International Journal for Numerical and Analytical Methods in Geomechanics*.

Wautier, A., Bonelli, S., Nicot, F., 2018. Flow impact on granular force chains and induced instability. *In preparation*

Analysis of suffusion for randomly distributed porosity and fines contents

J. Yang[1,2], Z.Y. Yin[2,3,*], P.-Y. Hicher[2] and F. Laouafa[1]

[1] INERIS, Verneuil en Halatte, 60550 France
[2] Research Institute of Civil Engineering and Mechanics (GeM), UMR CNRS 6183, Ecole Centrale de Nantes, 44300 France
[3] Key Laboratory of Geotechnical and Underground Engineering of Ministry of Education; Department of Geotechnical Engineering, College of Civil Engineering, Tongji University, Shanghai, 200092 China
**zhenyu.yin@ec-nantes.fr*

1 Introduction

Suffusion is a complex phenomenon appearing as a combination of detachment and transport of the finer particles driven by water flow, with possible filtration within the voids between coarser particles[1], which results in the degradation of soil strength[2-4]. This phenomenon has been widely studied experimentally and numerically over the last few decades [5-9]. In fact, soil nature are highly variable in space and then heterogenous in magnitude [10]. At the present time, few studies have been conducted to analyze the influence of variations of soil initial state (i.e. the initial porosity and the initial fraction of fines content) on the suffusion behaviors. In this paper, a thermodynamically consistent continuum model of suffusion is combined with the random field theory to investigate the erosion behavior of soil with spatially variable initial state of soil in one-dimensional condition.

2 Model formulations

The saturated porous medium is modelled as a material system composed of 4 constituents[11]: the stable fabric of the solid skeleton, the erodible fines, the fluidized particles and the pure fluid phase. The fines can behave either as a fluid-like (described as fluidized particles) or as a solid-like (described as erodible fines) material. Thus, a liquid-solid phase transition process has been accounted for in the present model by the introduction of a mass production term in the corresponding mass balances for erodible fines and fluidized particles.

The mass balances for the four constituents are reduced to the corresponding volume fraction balance:

$$\frac{\partial\left(n^i\right)}{\partial t}+\operatorname{div}\left(n^i\mathbf{v}^i\right)=\hat{n} \tag{1}$$

where i denotes the 4 constituents; n^i and $\mathbf{v}^i$ denote, respectively, the velocity of the corresponding constituent, $\hat{n}$ is the source term describing the exchange between the erodible fines and the fluidized particles.

$$\hat{n}=\hat{n}_e+\hat{n}_f \tag{2}$$

A model for the rate of the eroded mass $\hat{n}_e$ is given by the following relation[12]:

$$\hat{n}_e=-\lambda_e\left(1-\phi\right)\left(f_c-f_{c\infty}\right)\left|\mathbf{q}_\mathrm{w}\right| \tag{3}$$

where λ_e is the material parameter, $f_{c\infty}$ is the maximum fines content fraction after long seepage time, assumed to be decreased with the increase in the hydraulic gradient[13] :

$$f_{c\infty}=f_{c0}\left[\left(1-\alpha_1\right)\exp\left(-\alpha_2\left|\mathbf{q}_\mathrm{w}\right|\right)+\alpha_1\right] \tag{4}$$

The rate of the filtration is proposed as:

$$\hat{n}_f = \lambda_f \frac{\phi - \phi_{\min}}{\phi^{\beta}} c |\mathbf{q}_w| \tag{5}$$

where λ_f and β are the material parameters, $\phi_{\min}$ is the minimum porosity of soil.

In this study, the flow in the porous medium is governed by Darcy's law, the intrinsic permeability k of the porous medium depends on the current porosity ϕ and fines content fraction f_c. In our works we take the following expression [14]:

$$k = k_0 \left[1 - f_c (1 - \phi)\right]^{3m} \tag{6}$$

where m is the permeability parameter.

Eqs.(1)-(6) can then be extended to a system of partial differential equations in which the primary unknown variables are: the pore pressure, the porosity and the concentration of fluidized particles. It has been coded with MATLAB software [15] using a finite difference scheme.

3 Probabilistic analysis

The initial porosity ϕ_0 and the initial fraction of fines content f_{c0} are assumed to be lognormally distributed random variables. They are generated by the local average subdivision method which fully takes into account the spatial correlation, local averaging, and cross correlation. The generated random variables are mapped onto a finite-difference mesh and numerical simulations based on Monte Carlo method are performed.

The following parameters for both ϕ_0 and f_{c0} have been used for the probabilistic analysis in this study:(1) coefficient of variation ν: 0.05, 0.075, 0.1, 0.125, 0.15 and 0.175; (2) relative correlation length $\Theta = \theta / L$: 0.25, 0.5, 1.0, 2.0 and 4.0; (3) cross correlation coefficient ρ between ϕ_0 and f_{c0}: -1.0 and 1.0.

To keep accuracy and run-time efficiency, the sensitivity of results to the number of Monte Carlo simulations was examined. The results show that 2000 simulations are enough to give reliable and reproducible estimates.

Fig. 1 compares the probability of blockage during erosion with different uncertainties of ϕ_0 and f_{c0}.The probability of blockage during erosion is defined by counting the number of simulations in which the calculated hydraulic conductivity is smaller than its initial value, and then divided by the total number of simulations.

The results indicate that increasing the uncertainty in ϕ_0 and f_{c0} will always increase the probability of blockage during erosion. This can be explained by the fact that greater uncertainty leads to more dramatic changes in soil porosity and permeability at the interface of different layers, which in turn promotes the capture of the fine particles transported in water flow. Moreover, the ragged distributed ϕ_0 and f_{c0} with lower spatial correlation lengths make the layered system more inconsistent, and it, therefore, accelerates the formation of the filter cakes at the interface.

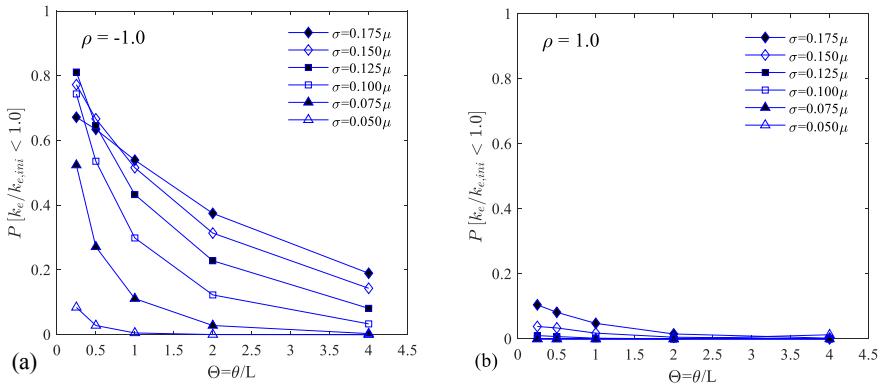

Fig. 1. 1D probabilistic results, comparison of probability of the appearance of blockage during erosion simulations: (a) ρ = -1.0; (b) ρ = 1.0

4 Conclusions

The influence of the initial state of soil characterized by its porosity and fine content on the erosion and filtration behaviors during suffusion process was investigated in this study. Probabilistic analysis shows that greater uncertainty leads to more dramatic changes of soil porosity and the permeability at the interface of different layers, which in turn promotes the capture of the fine particles transported in water flow. Higher spatial correlation length makes the layered system more uniform. However, the ragged distributed ϕ_0 and f_{c0} with lower spatial correlation lengths make the layered system more inconsistent. It leads to a rougher transition between the high erodible zones and the low erodible zones and, therefore, accelerates the formation of the filter cakes at the interface and increases the probability of blockage. Moreover, negatively correlated ϕ_0 and f_{c0} are more likely to cause blockage.

References

1. Bonelli, S., Marot, D.: On the modelling of internal soil erosion. In: *The 12th International Conference of International Association for Computer Methods and Advances in Geomechanics (IACMAG)*, pp. 7 pages.
2. Chang, C.S., Yin, Z.-Y.: Micromechanical modeling for behavior of silty sand with influence of fine content. *International Journal of Solids and Structures* 48, 2655-2667 (2011).
3. Yin, Z.-Y., Zhao, J., Hicher, P.-Y.: A micromechanics-based model for sand-silt mixtures. *International journal of solids and structures* 51, 1350-1363 (2014).
4. Yin, Z.-Y., Huang, H.-W., Hicher, P.-Y.: Elastoplastic modeling of sand–silt mixtures. *Soils and Foundations* 56, 520-532 (2016).
5. Reddi, L.N., Lee, I.-M., Bonala, M.V.: Comparison of internal and surface erosion using flow pump tests on a sand-kaolinite mixture. *Geotechnical Testing Journal* 23, 116-122 (2000).
6. Sterpi, D.: Effects of the erosion and transport of fine particles due to seepage flow. *International Journal of Geomechanics* 3, 111-122 (2003).
7. Bendahmane, F., Marot, D., Alexis, A.: Experimental parametric study of suffusion and backward erosion. *Journal of Geotechnical and Geoenvironmental Engineering* 134, 57-67 (2008).
8. Moffat, R., Fannin, R.J., Garner, S.J.: Spatial and temporal progression of internal erosion in cohesionless soil. *Canadian Geotechnical Journal* 48, 399-412 (2011).

9. Marot, D., Rochim, A., Nguyen, H.-H., Bendahmane, F., Sibille, L.: Assessing the susceptibility of gap-graded soils to internal erosion: proposition of a new experimental methodology. *Natural Hazards* 83, 365-388 (2016).
10. Dasaka, S., Zhang, L.: Spatial variability of in situ weathered soil. *Géotechnique* 62, 375 (2012).
11. Schaufler, A., Becker, C., Steeb, H.: Infiltration processes in cohesionless soils. ZAMM - *Journal of Applied Mathematics and Mechanics/Zeitschrift für Angewandte Mathematik und Mechanik* 93, 138-146 (2013).
12. Uzuoka, R., Ichiyama, T., Mori, T., Kazama, M.: Hydro-mechanical analysis of internal erosion with mass exchange between solid and water. In: *Proc. 6th International Conference on Scour and Erosion*, Paris, France, pp. 655-662. (Year)
13. Cividini, A., Bonomi, S., Vignati, G.C., Gioda, G.: Seepage-induced erosion in granular soil and consequent settlements. *International Journal of Geomechanics* 9, 187-194 (2009).
14. Revil, A., Cathles, L.: Permeability of shaly sands. *Water Resources Research* 35, 651-662 (1999).
15. Guide, M.U.s.: The mathworks. Inc., Natick, MA 5, 333 (1998).

Use of a particle model for studying coupled phenomena in the near well area for geothermal applications

M. Peter-Borie, V. H. Tran, A. Loschetter, A. Blaisonneau

BRGM, Orléans, FRANCE
m.peter-borie@brgm.fr

EGS (Enhanced/Engineered Geothermal System) constitutes a promising renewable energy technology to produce heat and electricity from deep geothermal energy. At several kilometers depth, the permeability of the system is generally naturally too low for economic exploitation of geothermal energy. Technologies are still a challenge as borehole stimulation are used to develop the system. Improving borehole stimulation effects needs a better understanding of the involved physical processes. In this paper, we focus on the thermal stimulation: the cooling of the rock from a cold fluid in the borehole, with or without overpressure, leads to induced fracturing. Drillers are interested in the injectivity index gain with stable borehole. In order to provide practical answers to them, questions related to the shape and growth speed of the induced fractures versus parameters as rock petrofabric or rock cooling velocity need to be answered. Moreover, induced fracture have to be translated into permeability gain. The complexity of involved phenomena (thermo-mechanical processes at the grain scale as well as at the borehole scale), as well as the need to quantify the extent of the failures lead us to use Discrete Element Method (DEM), and more specifically the bonded-particles model. Indeed, simulations at the granular phase level (micro scale) with DEM seem adapted to capture the thermo-mechanical processes induced by rock cooling in the near-borehole area and to understand the impact on the mechanical behaviour at metric scale. The code PFC2D (© Itasca Consulting Group) was used for the implementation of the DEM. In this paper, we focus on how the DEM can be used to help with real-case operations, and the theoretical aspects of this method will not be discussed. One can refer to Potyondy and Cundall (2004) for more information on particle-based methods.

I - Building the numerical rock model for simulations of thermal stimulation in wells

The elaboration of the numerical rock model setup is a preliminary essential task, often difficult due to insufficient data and thus high level of uncertainties. Before any numerical modeling, the real rock is conceptualized according to the role of each mineral phase in the behaviour of the rock (more details in Peter-Borie et al. 2011; Peter-Borie et al. 2015). The rocks involved in our investigations are grained, non-porous, and fully composed of crystallized minerals: each numerical particle represents a mineral grain or crystal in order to be able to catch the differential strain of the mineral under thermal loading (different thermal expansion coefficients). Parallel Bonds (PB) model the contacts between grains. The properties assignment is carried out with the purpose to ensure properties physically consistent at macroscopic and microscopic scales. Range of values for particles-grain properties are from literature review, and final values are from a calibration process that allows the fitting, at macro scale, to a real sample behaviour by carrying out set of numerical tests (triaxial, thermal conductivity and dilatation tests).

In the presented simulations, the calculation setup concerns a 2D plane perpendicular to the wellbore axis. The 2D approach is a constrained link to the computation capacity and time. Indeed, the definition of the near-wellbore setup needs to take into account an adequate extended area around the wellbore – at least three times the diameter of the wellbore to limit the impact of boundary conditions on the numerical results. A significant number of particles

are needed to build up such a large setup while keeping the size distribution close to the mineral size level. In order to push away the boundary conditions, the DEM near-wellbore model is embedded within a continuum mechanics based frame describing the region far away from the wellbore (FLAC, Itasca Consulting Group Inc., 2002).

The simulation of the stimulation is performed in three main steps (figure 1). The initial intact rock mass (only natural stresses) is firstly disturbed by the drilling of the well. In order to reproduce deconfining linked to borehole drilling, particles of the borehole are removed and forces are balanced. To simplify the numerical modeling setup, and to limit the computational time, the hydraulic pressure and the thermal loading are applied in two steps: hydraulic pressure is applied first, assuming that it acts instantaneously; the thermal loading is applied after, once the hydraulic pressure is fully installed. The fluid injection is assumed to act only on particles forming the wellbore surface. A specific procedure is used to detect a set of closed linked particles (connected by parallel bonds) around the wellbore. These particles are recorded in a specific list. The list of the wellbore particles is updated automatically when cracks appear between particles in the wellbore list. Hence, once the cracks start propagating from the wellbore, the injection pressure and the fluid temperature can penetrate into the crack as well.

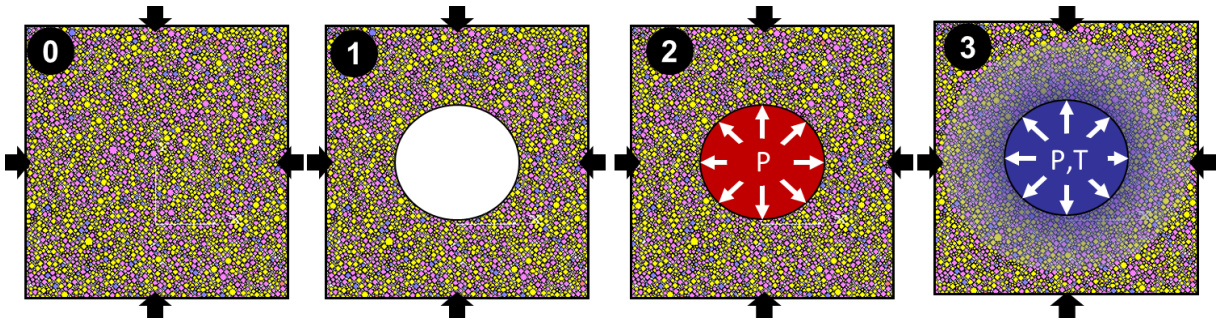

Figure 1 – Representations of the different steps of a simulation. 0. Application of the stress state on the numerical rock model. 1. Particles on the wellbore surface are removed to model drilling. 2. The hydraulic pressure is imposed in the wellbore. 3. The thermal loading is imposed. Black arrows symbolize the stress state. P represents the hydraulic pressure. T represents the thermal loading (cooling). The red color symbolizes the hot fluid, blue color the cold fluid.

II - Example of application: assessment of the thermal stimulation in the IDDP2 well

Following the above-described process, results of the simulation of the thermal stimulation of the IDDP-2 well in Iceland are presented. We focus on the assessment of the effect of the "speed" of cooling – numerically translated by the heat transfer coefficient. This coefficient results from the rock and the fluid intrinsic properties, and also from the fluid velocity in the well. As illustrated on figure 2, it appears that the heat transfer coefficient has a strong influence on the kinetics of crack apparition and on the tortuosity of the connected crack path.

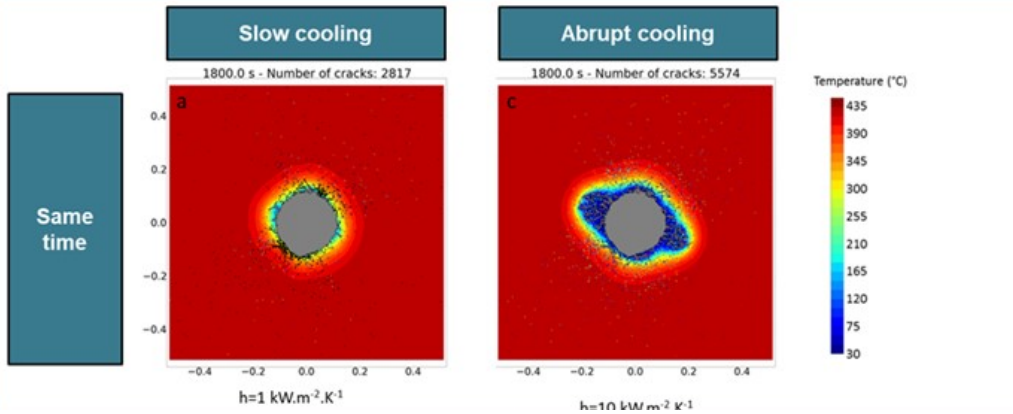

Figure 2 –Influence of the heat transfer coefficient on the temperature field and on crack apparition.

III - First thoughts for introducing cracks into description of permeability evolution

The challenge is then to translate the simulated rock damaging into permeability evolution of the rock. From the results of numerical simulation of the thermal stimulation, a method of estimation of permeability evolution in the near-wellbore is in progress. Considering that the rock permeability increases with the apparition of thermomechanical cracks, we propose to evaluate on the one hand the permeability in the rock matrix linked to all the cracks, and, on the other hand, the permeability of newly created fracture by crack coalescence. For both cases, in the initial state, we assume that the permeability of the medium k_d^{ini} is constant. At the cracking state, rock permeability in a domain k_d is determined by the sum of the initial permeability k_d^{ini} and the permeability of the microcracks k_d^{crk} :

$$k_d = k_d^{ini} + k_d^{crk}$$

The permeability of cracks k_d^{crk} is estimated by the Poiseuille law in the "local domains" (Zhou et al., 2016). The "local domains" are established by the connectivity of the particles of the numerical model. Assuming that cracks in a domain are connected, we can determine the propagation of fractures from the wellbore into the rock.

Limits and perspectives

The DEM approach seems to be fairly adapted to catch most of the processes at micro and macro scale of a thermal stimulation in a non-porous grained rock as mostly encountered in the deep geothermal system. But the numerical rock setup as well as the simulation need important computation capacity and time. As a consequence, at this time, this approach cannot be used for a daily support of the operations on site, but only for upstream researches or investigations of the feedback. Another consequence of the computational constraints is that simplifications are made to save time: 2D approach whereas permeability linked to new fracture pathway is a 3D problem, decoupling the hydraulic pressure from the thermal loading… Solutions and improvements are still sought.

Acknowledgement

This study is the results of several projects, included:
- the "Prochepuits" project, funded by the ANR ANR-07-PCO2-0 (numerical rock model)
- Internal BRGM projects (NUMROCH and CAPTAIN) (numerical rock model)

- the DEEPEGS project, which received funding from the European Union HORIZON 2020 research and innovation program under grant agreement No 690771 (results of the TM modelling)

References

Peter-Borie M, Blaisonneau A, Gentier S, et al (2011) A particulate rock model to simulate thermo-mechanical cracks induced in the near well by supercritical CO2 injection. In: *IAMG 2011 : the Annual Conference of the International Association for Mathematical Geosciences*. Salzburg, Austria, pp 141–148

Peter-Borie M, Blaisonneau A, Gentier S, et al (2015) Study of Thermo-Mechanical Damage around Deep Geothermal Wells : from the Micro- Processes to Macroscopic Effects in the Near Well. *Proc World Geotherm Congr* 19–25.

Potyondy DO, Cundall P a. (2004) A bonded-particle model for rock. Int J Rock Mech Min Sci 41:1329–1364. doi: 10.1016/j.ijrmms.2004.09.011

Zhou J., L. Zhang and Z. Pan (2016) Numerical investigation of fluid-driven near-borehole fracture propagation in laminated reservoir rock using PFC 2D, *Journal of Natural Gas Science and Engineering*, pp. 36, 719-733, 2016.

On the role of pore pressure in dynamic instabilities of saturated model granular materials

T.T.T. Nguyên*, T. Doanh*, A. Le Bot & D. Dalmas****

**Ecole Nationale des Travaux Publics de l'Etat. LTDS (UMR CNRS 5513).*
2 Rue M. Audin, 69518 Vaulx en Velin Cedex. France.
*** Ecole Centrale de Lyon. LTDS (UMR CNRS 5513).*
36 avenue Guy-de-Collongue, 69134 Ecully Cedex. France.
thiep.doanh@entpe.fr

The behaviour in drained isotropic and triaxial compression of loose, fully saturated monodisperse glass beads assembled by the moist tamping and undercompaction method reveals the ubiquitous presence of dynamic instabilities, previously unknown in granular mechanics. These instabilities (i.e. isotropic collapse, compression stick-slips, and especially isotropic liquefaction) exhibit one common unexpected component in the sudden surge of excess pore pressure.

Figure 1(left) shows the typical compressibility under isotropic consolidation from 20 to 500 kPa with four isotropic collapses under undetermined triggering stress and figure 1(right), the temporal evolution of static and dynamic pore water pressure of the fourth collapse at 451 kPa, measured simultaneously at sample top and bottom by two different measurement techniques (piezoresistive and piezoelectric). The static pore pressure at the sample top (blue full line) commences with a sudden surge from constant back-pressure, followed by a rapid dissipation from a short-lived stable state within a few seconds towards the equilibrium state of back-pressure. The bottom static pore pressure (green full line) rises up earlier. A smaller stabilised excess bottom pore pressure is briefly obtained despite a completely open drainage system at the bottom platen. The small variation of the bottom pore pressure is probably linked to the open end of the drainage system and the large oscillated phase of the top pore pressure to the dead end of the top cap drainage. The complementary dynamic measurements (dashed lines) follow exactly the static ones in the transient phase, confirming the validity of these pore pressure measurements.

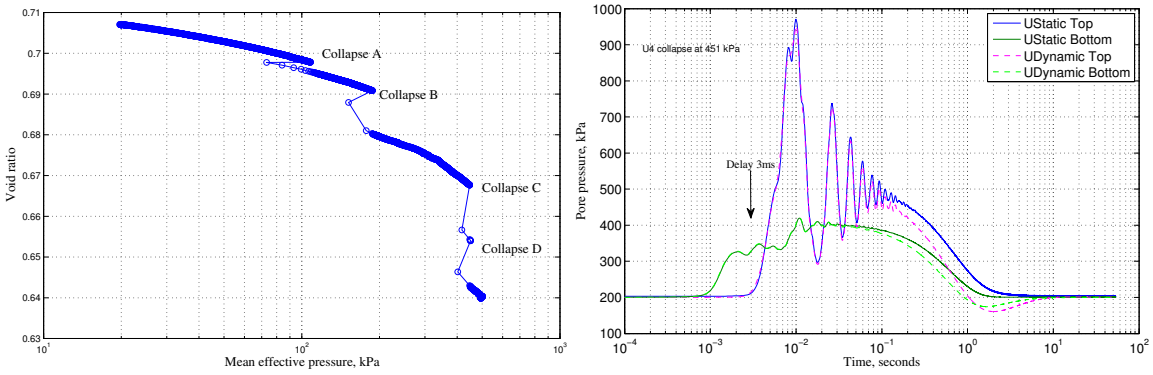

Figure 1. Isotropic instabilities from 20 to 500 kPa of confining pressure : (left) compressibility; (right) temporal evolution of dynamic and static pore pressure at sample top and bottom of isotropic collapse at 451 kPa.

These measurements indicate a local liquefaction due to large pore pressure peaks and a briefly non-homogenous effective stress state of less than one second. Unexpected isotropic liquefaction occurs if the stabilised excess pore pressure can be maintained for more than one second (Doanh et al., 2014). Similar results have been obtained for drained stick-slips under triaxial compression with constant cell pressure.

Figure 2(left) shows a highly correlated relationship between the stabilised top excess pore pressure and the incremental volumetric strain during the isotropic collapse and during the slip component, in a usual semi-logarithmic scale in soil mechanics; and figure 2(right) the effects of dynamic excess top pore pressure peaks. These figures show the control of the short-lived pore pressure peaks on the mechanical behaviour of the dynamic consolidation under constant deviatoric stress. In the stick-slip experiment, the stabilised excess pore pressure is in turn controlled by the normalised deviatoric stress drop.

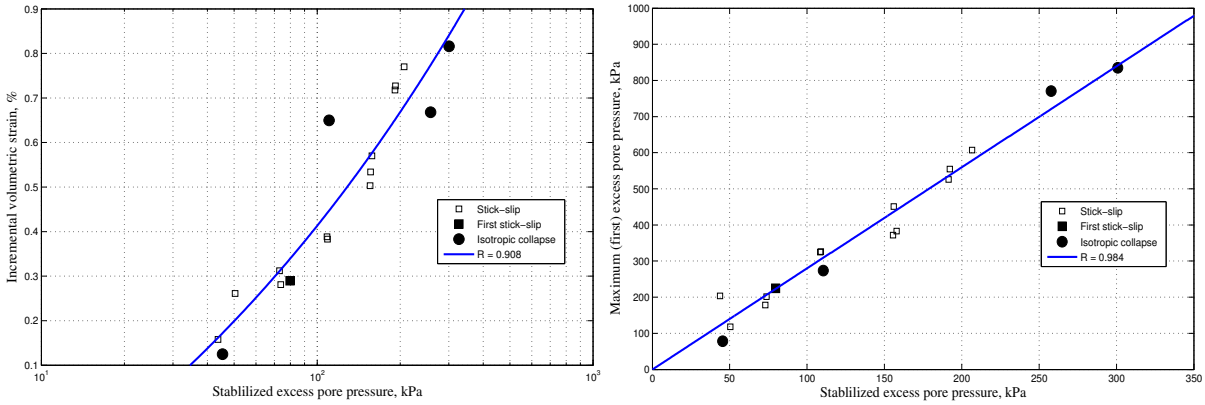

Figure 2. Effects of dynamic stabilized excess pore pressure on : (left) incremental volumetric strain; (right) dynamic excess pore pressure peaks.

The sudden surge of interstitial pore fluid is not the primary cause of the observed instabilities, since a dry assembly of model granular materials produces the same stick-slip phenomenon in triaxial compression (Adjemian et al., 2004; Alshibli et al., 2006). Nevertheless, how this excess pore pressure is generated, oscillated, propagated and maintained for a prolonged period of time of some seconds in the case of isotropic liquefaction is still a mystery, as well as how these mechanisms are triggered. The most reasonable though imprecise scenario points to a possible dynamical collapse of the granular structure triggered by a spontaneous failure of the force chains, generating an instantaneous surge of excess pore pressure in a fully saturated system.

References

1. Adjemian, F., Evesque, P. Experimental study of stick-slip behaviour. *Int. J. Num. Ana. Meth. in Geom.*, 28(6):501–530, 2004.
2. Alshibli, K.A., Roussel, L.E. Experimental investigation of stick-slip behaviour in granular materials. *Int. J. Num. Ana. Meth. in Geom.*, 30(14):1391–1407, 2006.
3. Doanh, T., Le Bot, A., Abdelmoula, N., Hans, S., Boutin, C. Liquefaction of immersed granular media under isotropic compression. *Europhys. Lett.*, 108(2):24004, 2014.

Merging criteria for pores and constrictions

F. Seblany* & U. Homberg[+] & E. Vincens* & P. Winkler & K.J. Witt****

** University of Lyon, Ecole centrale de Lyon, France*
*** Bauhaus-Universität Weimar, Germany*
[+] Zuse Institute Berlin, Germany
eric.vincens@ec-lyon.fr

A granular medium includes a set of large volumes of voids between solid particles (pores) connected by throats. The narrowest sections in these throats are generally denoted as constrictions. Then, pores and constrictions constitute a partition of the void space helpful to defining, respectively, its morphology and its topology. There are different techniques for pore space characterization: through experiments, using analytical approaches or numerical approaches. A synthesis of these different approaches can be found in (Vincens et al., 2015). The Discrete Element Method combined with spatial partitioning techniques (Delaunay tessellation or Voronoï diagram, among others) can be helpful for deriving general tendencies in case of spheres.

In the Delaunay tessellation, the primary definition for a local pore is the Delaunay cell, i.e. a tetrahedron which vertices are located at the centers of spherical particles. Constrictions are found on the four faces of each tetrahedron and a definition for them is chosen as the largest empty discs that can be inscribed between the three particle vertices of a tetrahedron face (Al Raoush et al., 2003; Reboul et al., 2008) (Figure 1). Eventually, the inscribed void sphere between the four particles, vertices of a Delaunay cell is computed and can be considered as a characteristic of the morphology of that cell.

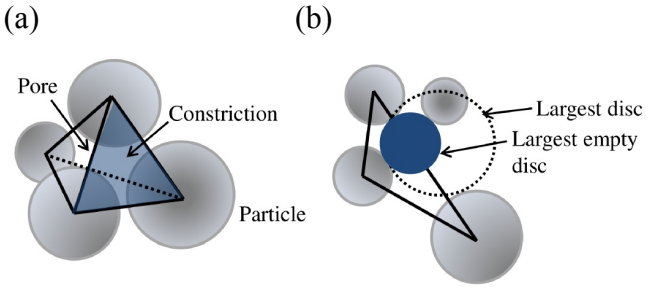

Figure 1: (a) Tetrahedron built from the centers of four neighboring spheres; (b) Definition of a constriction: the largest disc included in the void space for a given face

Due to the duality of Delaunay and Voronoï decompositions, the Voronoï nodes should correspond to the centers of the inscribed void spheres of the Delaunay tetrahedra and their distance to the surrounding solid spheres to the radius of these inscribed void spheres. When applying a Voronoï computation that is based on the Euclidean distance to the solid spheres as described by Lindow et al. (2011), the edges between the Voronoï nodes are curved and run along the maximal distance to the surrounding solid spheres. Then, they describe the median path joining pore centers. The centers of constrictions are located where the distance to the surrounding spheres is minimal along the edge (Figure 2).

Since both derived partitions of the void space are somehow artificial, the question arises of whether an excessive partition of the void space is generated by both mathematical techniques

and how to handle it. Indeed, using a Delaunay tessellation, Al-Raoush et al. (2003) found that two inscribed void spheres attached to these two neighboring tetrahedra may overlap. It signifies that the opening size between two adjacent tetrahedra may be high enough to indicate a strong interconnection between them. For the same reason, Homberg et al. (2012) considered that merging two adjacent pores may be required when the size of the constriction linking these pores is very close to the smallest pore size (pore separation approach).

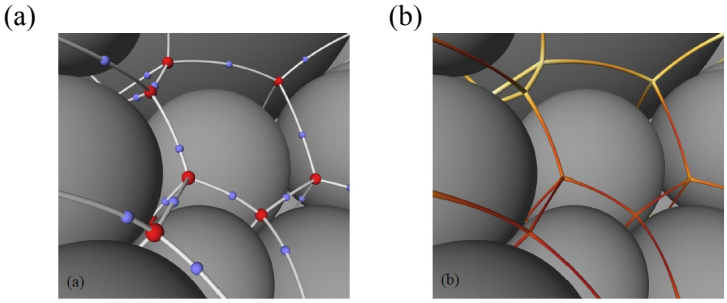

Figure 2: (a) Detail of a Voronoï graph; (a): red spheres at crossing indicate the centers of pores, while the blue spheres represent the centers of constrictions on the edges; (b) The diameter is color-coded along the edges with yellow (large) to red (small)

The aim of this work has been to find the correspondence between two merging criteria, one based on the overlapping inscribed void sphere (technique A) and the other related to the pore separation approach (technique B). A loose sample composed of spheres with the grading involved in (Vincens et al., 2015) was created within the Yade code (Šmilauer et al., 2010). For technique A, three levels of merging are proposed: L0 which is the direct computation from the weighted Delaunay tessellation, L1, where merging involves only direct neighbors with overlapping inscribed void spheres and L2, where are added the neighbours of the neighbours if their inscribed void spheres overlap too. The number of merged pores is then limited. In the case of technique B, a threshold t must be defined: for adjacent pores with inscribed void spheres of size *dpi* and *dpj*, they are merged if the diameter of the constriction between them is greater than *(1-t)*min(dpi;dpj)*. In this case, there is no limited number of merged pores if t is high enough.

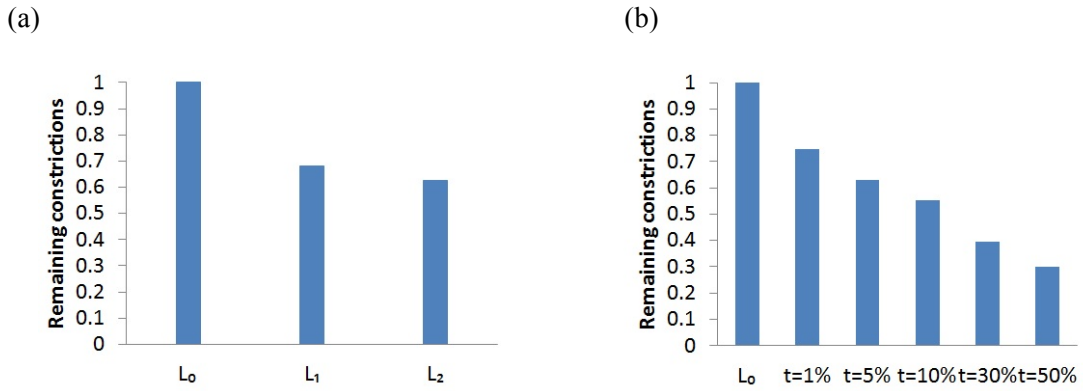

Figure 3: Remaining constrictions after merge: (a) overlapping inscribed void sphere technique, pore separation technique

For the studied sample, technique A tends to limit the possibility for merging and L2 does not bring about new features compared to L1 (Figure 3). In the case of technique B, there is always an evolution when t increases. For a high enough value of t, the void space can merge

into a single pore. It is not desirable to arrive to such a situation where the pores no longer have a local definition. L1 or L2 merging intrinsically avoid this drawback.

In Figure 4, the constriction size distributions for L0 and for merging techniques A and B are depicted where merging allows a clear single model to appear. This mode is not affected by the kind of merging (L1; L2) neither by the value of the threshold if *t* remains smaller than 10%.

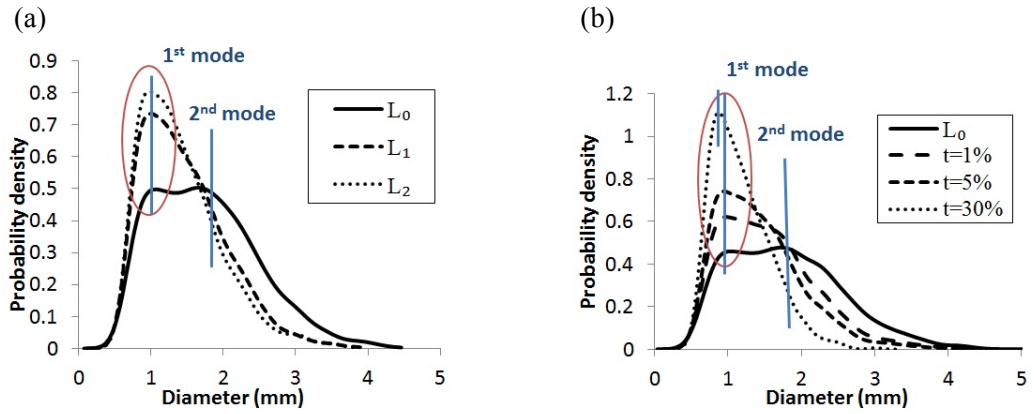

Figure 4: Constriction size distributions for different merging cases; (a) overlapping inscribed void sphere technique, pore separation technique

The L1 cumulative constriction size distribution can be obtained by choosing t equal to 2% irrespective of the density. In a same manner, L2 cumulative constriction size distribution can be obtained by choosing *t* equal to 5%. The same findings hold true for the cumulative distribution of inscribed void spheres.

References

Vincens E., Witt K.J., Homberg U., 2015. Approaches to determine the Constriction Size Distribution for understanding filtration phenomena in granular materials. *Acta Geotechnica,*10(3), pp. 29-303.

Al-Raoush, R., Thompson, K., Willson, C.S., 2003. Comparison of network generation techniques for unconsolidated porous media. *Soil Science Society of America Journal,* 67(6), pp. 1687-1700.

Reboul, N., Vincens, E., Cambou, B., 2008. A statistical analysis of void size distribution in a simulated narrowly graded packing of spheres. *Granular Matter*, 10(6), pp. 457-468.

Lindow, N., Baum, D., Hege, H. C., 2011. Voronoï-based extraction and visualization of molecular paths. *IEEE Transactions on Visualization and Computer Graphics*, 17(12), pp. 2025-2034.

Homberg, U., Baum, D., Prohaska, S., Kalbe, U., Witt, K.J., 2012. Automatic extraction and analysis of realistic pore structures from CT data for pore space characterization of graded soil. In: *Proceedings of the 6th International Conference Scour and Erosion (ICSE-6),* pp. 66-73.

The modelling of mechanical degradation in quasi-brittle systems: between the continuous and discontinuous standpoints

N. Moës

Ecole Centrale de Nantes, GeM Institute UMR CNRS 6183,
1 rue de la Noe, 44321 Nantes, France, nicolas.moes@ec-nantes.fr

We consider the quasi-brittle failure of structures under quasi-static loading. At some point in the loading path, the structure enters into a dynamic regime because a stable quasi-static state does not exist anymore. When entering the dynamic regime, a macro crack develops (this being the main difference between quasi-brittle and brittle failure for which a dynamic regime occurs prior to the development of any macro cracks). An important characteristic of the quasi-brittle failure is that it produces an important size effect. The stress (applied force divided by the area on which the load is applied) at failure depends on the size of the specimen. Note that this size effect is quite different from the Weibull size effect in brittle failure.

Let us consider different theories for modelling failure and discuss if they are well suited for quasi-brittle failure.

The Griffith theory is a well-known discontinuous approach. The theory predicts the advance of an existing crack based on energetic considerations. The crack advances if the energy release rate reaches a limit value called the crack toughness. This theory is not well suited for quasi-brittle failure for two main reasons. First, it requires an existing crack to be applied and, second, it does not exhibit the proper size effect (because the Griffith model does not contain a length).

The cohesive model is also a discontinuous approach. The tractions on the crack faces do not vanish immediately as the crack advances but are related to the crack opening. A cohesive zone (non-zero tractions) thus exists in the wake of the mathematical crack tip. This model predicts the proper size effect (because it contains a length), but is unable to incorporate the triaxiality effect. The model is based on the normal stress on the crack lips and not based on the full stress (or strain) tensor. It is thus unable to predict properly splitting cracks, for instance.

Regularized damage models are continuous models. One can place in this category non-local integral approaches, gradient damage, phase-field or variational fracture approaches. These models do contain a length, but are not tailored to directly exhibit displacement jumps. The displacement jump is smeared. This is why these approaches are usually coined diffuse approaches. Even though they contain a length, the capability of diffuse approaches to predict the proper size effect is still an open question.

More recently, a new model has been proposed which gathers discontinuous and continuous ingredients (Moës et al. 2011). It is called the Thick Level Set (TLS) approach to fracture. Regarding the continuous ingredient, a boundary (called localization front) separates the local damage zone to the non-local damage zone. This is a novelty compared to standard diffuse approaches, since the regularization is only active where needed. This reduces dramatically the overcost of the regularization. Concerning the discontinuous ingredient, within the non-

local zone, displacement discontinuities are activated at points which lie farther than some distance from the localization front. The damage value inside the non-local zone is given as a function of the distance to the front. For some critical length, this value is set to one (fully degraded material). The set of points for which the damage is equal to one forms the crack and, on this crack, the displacements are allowed to be discontinuous. In practice, the discontinuity is introduced with the extended finite element method (X-FEM).

Even more recently, we managed to introduce a cohesive crack prior to the full damage of the material. This opens the possibility of combining cohesive and bulk capabilities in a concurrent manner (interesting feature for crack growth under shear and friction). Details on this Thick Level Set version, coined V2, are given in (Le et al. 2008). Figure 1 shows the rising complexity (with richer modelling capabilities) from the cohesive to the Thick Level Set approach (V1 then V2).

To summarize, the Thick Level Set approach allows combining the advantages of the discontinuous and diffuse approaches to fracture.

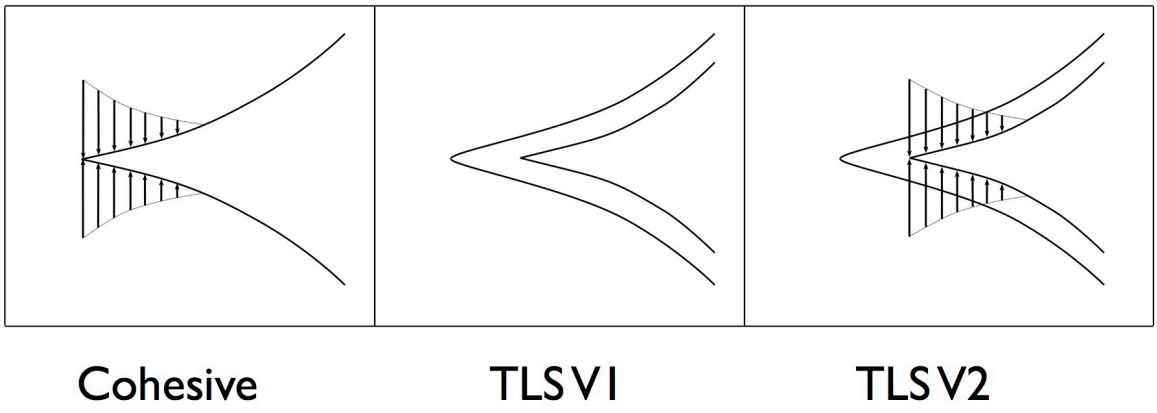

Figure 1. Different crack representations, from left to right: cohesive model, thick level set model and finally the thick level set incorporating cohesive degradation.

References

Moës, N., Stolz, C., Bernard, P.-E., & Chevaugeon, N. (2011). A level set based model for damage growth : the thick level set approach. *International Journal For Numerical Methods in Engineering*, 86, 358–380.

Lé, B., Moës, N., & Legrain, G. (2018). Coupling damage and cohesive zone models with the Thick Level Set approach to fracture. *Engineering Fracture Mechanics*, 193, 214–247. http://doi.org/10.1016/j.engfracmech.2017.12.036

Acoustic Emission Analysis of Damage Process in Cobourg Limestone

S.Y. Alam [1], A.P.S. Selvadurai [2], F. Grondin [1], P.-Y. Hicher [1]

[1] Research Institute of Mechanics and Civil Engineering (GeM), UMR CNRS 6183
Ecole Centrale de Nantes, France
[2] Department of Civil Engineering and Applied Mechanics
McGill University, Canada
syed-yasir.alam@ec-nantes.fr

Abstract
The Cobourg limestone has a dominant fabric consisting of a fine-grained light grey nodular fraction composed of carbonates separated by a darker limestone, referred to as argillaceous partings. The limestone is the proposed host rock for a Low and Intermediate Level Waste Deep Geologic Repository (DGR) at the Bruce nuclear site at Kincardine and a potential host rock for the deposition of used fuel under the APM program. The evolution of permeability at excavation damage zones in the vicinity of repository openings located at depth is therefore of importance to the environmental impact assessment. Acoustic Emission technique is used to map damage evolution within cylindrical samples of the Cobourg Limestone measuring 150 mm in diameter and 300 mm in length. These represent the largest specimens of Cobourg Limestone tested to date and provide a basis for establishing the influence of the internal scale of the heterogeneities.

Introduction

The Cobourg Limestone displays heterogeneity resulting from the interspersed fabric of a calcite, dolomite rich light gray, nodular limestone separated by dolomitic-calcitic-argillaceous partings. There is some visual evidence of a nominal plane of stratification but this can vary from sample to sample depending on the spatial arrangement of the fabric. The rock with observable heterogeneity in sample scale has a fine-grained matrix of carbonate, shale and fossiliferous material ranging in size from 2 to 8 mm. The limestone minerals form nodules (10 to 50 mm diameter) of a light gray colour, which are interspersed by thin discontinuous regions of a darker coloration, similar to shale, containing the clay minerals.

Experimental Setup

The fabric of the argillaceous limestone is very similar to that of a weak concrete; preliminary tests indicate the development of failure at the weaker argillaceous partings of the rock that can enhance the permeability. The unconfined compression testing of one 150 mm diameter and 300 mm height sample of the Cobourg Limestone is performed using a universal testing machine of 300 kN capacity. The specimen is loaded up to 30% of UCS (Unconfined strength) which is about 530 kN. The loading level corresponds to the similar tests carried out in Enviromental Geomechanics Laboratory at McGill University in order to characterize the permeability of the geomaterial. The loading is applied with a uniform displacement of the loading platen.

In this study, growth of fracture zone is investigated using synchronized observation of acoustic emissions (AE). The technique allows a continuous and a real time data acquisition and thus the damage evolution during the load test can be recorded. The AE system comprised of an eight channel AEWin system, a general-purpose interface bus (2 x PCI-DISP4 having 4 channels each) and a PC for data storage analysis. A 3D analysis with an AEWin algorithm is performed for the localization of AE events. 8 piezoelectric sensors were

used. The transducers were placed around the specimen to minimize errors in the AE event localization. The signals as detected by sensors were amplified by an amplifier with a gain of 40 dB. A detection limit of 35 dB was chosen to filter background noise (RILEM TC212 2010). The acquisition system was calibrated before the test using a pencil lead break procedure HSU-NIELSEN (RILEM TC212 2010). The acoustic wave propagation velocity measured in this study was 2800 m/sec. The descriptors were further analyzed and evaluated with Noesis® software.

Damage localization

During the formation of a crack, energy is emitted as an elastic wave and propagates from the crack location to the AE transducers at specimen surface. The localization map of AE events is based on arrival times of the first wave at each transducer and their respective velocity in rock specimen. Once the arrival time is picked, least-square method is used to estimate the event location. Though damage accumulation with AE technique was detected in 3D, the cumulative acoustic events are also placed in 2D. The detected AE events are presented over a window covering the specimen height 300 mm and a diameter 150 mm. Each plotted point indicates a detected AE source.

It is evident from the localization map that specimen undergoes damage during the loading test. The damage is distributed mostly in the upper part of the specimen. By examining the sample, cracks are also noticed in the upper part of the specimen. Although the loading is in the elastic range, damage occurs due to strong heterogeneity in the material. The source of the damage cannot be known in this localization map. The identification of source and nature of damage will be performed after statistical analysis of the AE parameters.

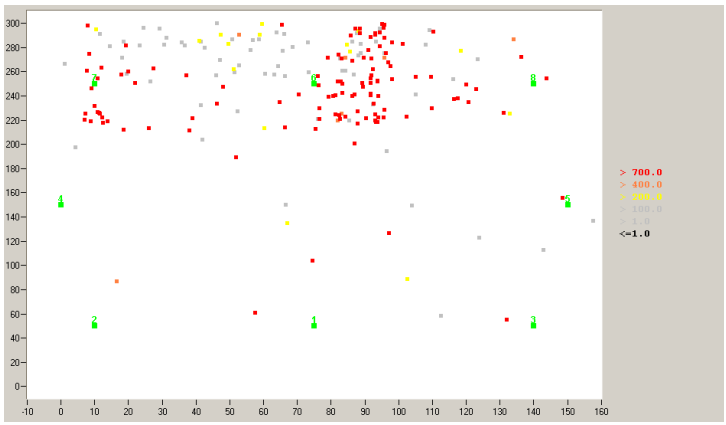

Figure 1: 2D view of AE events localization map with energy discretization

In addition to number of events, it is very important to investigate AE signal parameters. The initiation and propagation of cracks in geomaterials are generally correlated to the study of AE signals of certain amplitude. Extensive studies have shown that the absolute acoustic energy is the most important parameter to characterize an event (Muralidhara et al. 2010; Hadjab et al. 2007). Events with the highest energy level usually a significant crack can be observed in Figure 1.

During the initial loadings, no AE activity is noticed, however at about 50 secs of loading, both AE Energy and AE hits begin to increase. It can be observed that the increase is not uniform and sudden jumps are noticed which is related to material damage process which may include fracturing at argillaceous partings, sliding, shearing or crack openings. Few sensors (2, 4 and 5) register low AE hits and energy as they are far from the damage location. The damage activity in Cobourg specimen is very similar to damage activity in other quasi-brittle materials like concrete which show the same order of energy release due to the fracture

process.

Statistical Analysis of AE parameters

In this study, based on a hierarchical dendrogram, the classification of AE data was realized with the non-supervised K-means method that is associated with the principal component analysis (PCA). Six parameters with a correlation level less than 0.95 have been chosen: Rise Time, Counts to Peak, Counts, Duration, Amplitude, Average Frequency and Absolute Energy. In order to impose an equivalent weight factor to each AE component, all the descriptors were normalized in the interval of [-1 1]. Two clusters are distinguished [0] and [1] which indicates two classes of AE activity (Figure 2). It allows better visualization of the temporal characteristics of signals and displaying groups of AE activity corresponding to each nature of material failure.

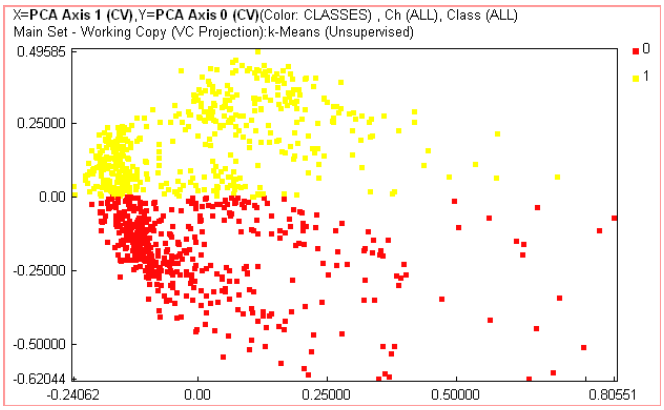

Figure 2: Identification and visualization of classes from Principal Component Analysis

Crack classification is necessary to identify the fracture phenomenon occurring in the rock specimen. One method to classify the crack is the combination of average frequency and RA values RA value is a calculated feature derived from Ride time divided by Amplitude showing the reciprocal of gradient in AE signal wave forms, which is reported in ms/V.From these two parameters, cracks are readily classified into tensile and shear cracks. This crack classification method is based on the JCMS-III B5706 code. Class 0 cracks mostly belong to shear zone however, class 1 cracks belong to both shear and normal cracks.

Magnitude of cracking as previously said can be estimated based on two parameters: Peak amplitude and Absolute Energy. Peak amplitude is closely related to the magnitude of source event. It can be observed that class 0 cracks have higher amplitude thus a higher magnitude of cracking occurs here. One of the preferred parameter to interpret cracking magnitude is Absolute Energy of Acoustic Wave as it is sensitive to both amplitude and duration and less dependent on the voltage threshold and operating frequencies. It can be observed that Class 0 events are significantly higher in absolute energy as compared to class 1 event. Both classes of cracks are formed throughout the loading history.

References

Muralidhara S., Raghu Prasad B.K., Eskandari H. and Karihaloo B. (2010). Fracture process zone size and true fracture energy of concrete using acoustic emission. *Construction Building Materials*. 24:479-486.

Hadjab H.S., Thimus J.F. and Chabaat M. (2007). The use of acoustic emission to investigate fracture process zone in notched concrete beams. *Curr Sci*. 93(5):648-653.

A variational scheme for damaged elasto-plastic springs and application to granular micromechanics of cohesive materials

L. Placidi *,**, E. Barchiesi **,**** & A. Misra ***,******

**Facoltà di Ingegneria. Università Telematica Internazionale Uninettuno*
Email: luca.placidi@uninettunouniversity.net
*** Dipartimento di Ingegneria Strutturale e Geotecnica*
Università degli Studi di Roma "La Sapienza"
Email: barchiesiemilio@gmail.com
****The University of Kansas.*
Civil, Environmental and Architectural Engineering Department
Email: amisra@ku.edu
***** International Research Center*
on Mathematics and Mechanics of Complex Systems

Granular materials span the spectrum from highly consolidated dense solids formed of particulate precursors to confined packing of non-cohesive particles. They possess granular texture and can be described as conglomeration of atomic to larger sized grains.

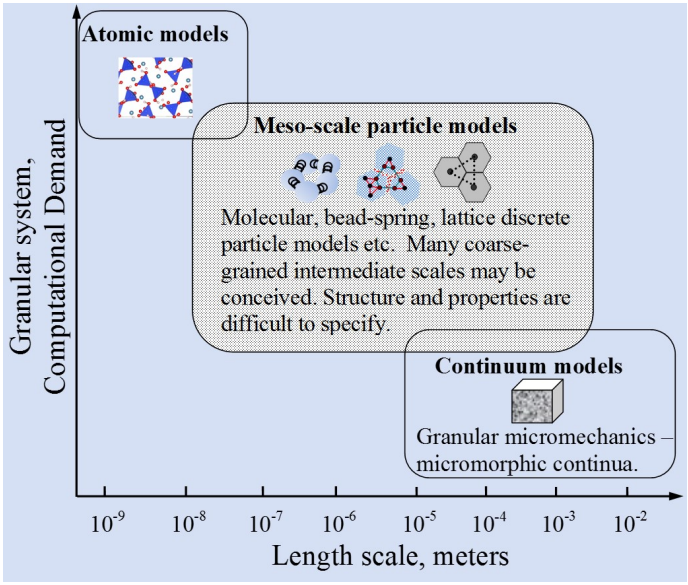

Figure 1. Scales

They share the common trait in that their behavior at the macro-scale, containing a large number of grains ($> 10^6$), is profoundly affected by the grain-scale interactions.
In all their forms, these materials are characterized by complex structures and compositions (mostly indeterminable). For many problems in engineering and science, a continuum description of their mechanical behavior is desirable.
The challenge is to develop continuum models founded upon a sound theoretical consideration that (i) represents micro-scale effects of grain interactions, (ii) describes mechanical properties at scales amenable to continuum approaches able to replicate materials'

unique behavior traits (such as strain softening, pressure-dependency, inherent and loading induced anisotropy, localized strains and fractures), and (iii) has far fewer computational needs than that of other grain-based approaches, such as DEM or MD (which have their own issues).
We focus upon a non-classical enhanced continuum model that can capture the effects of micro-scale mechanisms. Granular Micromechanics are summarized as follows:
1) Identification of grain (micro-scale) motions in terms of the continuum (macro-scale) deformation measures.
2) Expression of the continuum (macro-scale) energy density in terms of the volume average of inter-granular deformation energy (micro-scale energy).
3) Derivation of the constitutive relations, variational principle, balance equations and boundary conditions.

A granular material framework has, therefore, been described, as well as a new discrete model, see Fig. 2, with a variational procedure. Finally, standard simulation can be reproduced.

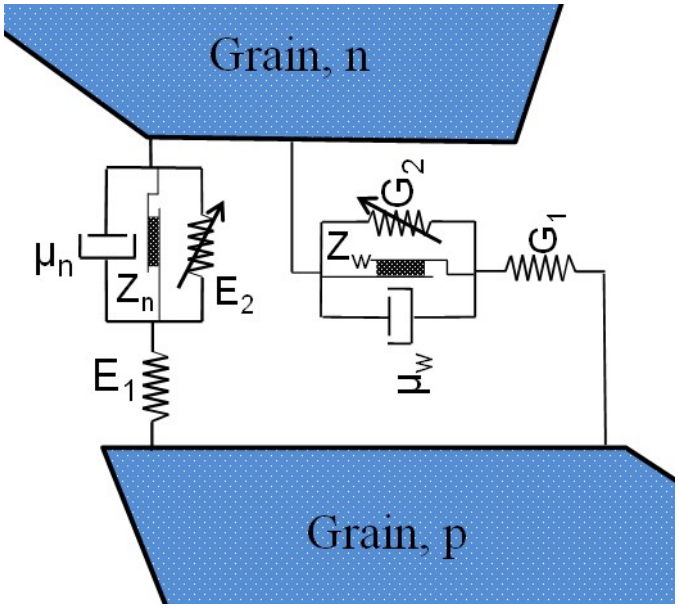

Figure 2. Grain interactions

Among the general aspects of granular materials, we have discussed a constitutive theory framework. In particular, a variational inequality principle and a new damaged elastoplastic spring model. On the basis of this framework, illustrated by the papers of the reference list, we have shown numerical simulations for both quasi-static and dynamic cases.

In this presentation we have also discussed some outlooks such as:

1. Performing the homogenization with the new discrete model for springs.
2. Performing the continuum simulation with a standard target continuum model and with a non-standard target continuum model, e.g. second gradient, micromorphic etc.
3. Exploiting a method for the experimental characterization of the newly introduced constitutive coefficients.
4. Exploiting the 3D case.

References

A. Misra, L. Ouyang, J. Chen, and W.Y. Ching. Ab initio calculations of strain fields and failure patterns in silicon nitride intergranular glassy films. *Philosophical Magazine*, 87(25):3839-3852, 2007.

Y. Yang, W.Y. Ching, and A. Misra. Higher-order continuum theory applied to fracture simulation of nanoscale intergranular glassy lm. *Journal of Nanomechanics and Micromechanics*, 1(2):60-71, 2011.

Y. Yang and A. Misra. Micromechanics based second gradient continuum theory for shear band modeling in cohesive granular materials following damage elasticity. *International Journal of Solids and Structures*, 49(18):2500-2514, 2012.

A. Misra and V. Singh. Micromechanical model for viscoelastic materials undergoing damage. *Continuum Mechanics and Thermodynamics*, 25(2-4):343-358, 2013.

A. Misra and V. Singh. Thermomechanics-based nonlinear rate-dependent coupled damage-plasticity granular micromechanics model. *Continuum Mechanics and Thermodynamics*, 27(4-5):787-817, 2015.

Antonio Rinaldi, Placidi L (2015). A microscale second gradient approximation of the damage parameter of quasi-brittle heterogeneous lattices. *Zeitschrift für Angewandte Mathematik und Mechanik*, vol. 94, p. 862-877, ISSN: 0044-2267, doi: DOI: 10.1002/zamm.201300028

Placidi L (2015). A variational approach for a nonlinear 1-dimensional second gradient continuum damage model., *Continuum Mechanics and Thermodynamics,* vol. 27, p. 623-638, ISSN: 0935-1175, doi: 10.1007/s00161-14-0338-9

Placidi L (2016). A variational approach for a nonlinear one-dimensional damage-elasto-plastic second-gradient continuum model. *Continuum Mechanics and Thermodynamics*, vol. 28, p. 119-137, ISSN: 0935-1175, doi: 10.1007/s00161-014-0405-2

A. Misra and P. Poorsolhjouy. Granular micromechanics based micromorphic model predicts frequency band gaps. *Continuum Mechanics and Thermodynamics*, 28(1-2):215234, 2016.

A. Misra and P. Poorsolhjouy. Granular micromechanics model of anisotropic elasticity derived from gibbs potential. *Acta Mechanica*, 227(5):1393-1413, 2016.

Kezmane A., Chiaia, B., Kumpyak, O., Maksimov, V., Placidi L (2017). 3D Modeling of reinforced concrete slab with yielding supports subject to impact load. *European J. Environmental and Civil Engineering*, vol. 21, p. 988-1025, ISSN: 1964-8189, doi: 10.1080/19648189.2016.1194330

Placidi L, Barchiesi Emilio (2018). Energy approach to brittle fracture in strain gradient modelling. *Proceedings – Royal Society. Mathematical, Physical and Engineering Sciences*, vol. 474, 20170878, ISSN: 1471-2946, doi: 10.1098/rspa.2017.0878.

Towards the design of an enriched concrete with enhanced dissipation performances

I. Giorgio* & D. Scerrato*

**International research center for the Mathematics and Mechanics of complex systems, M&MoCS*

A continuum model for concrete is developed as a microstructural medium (see Scerrato et al. 2014) in order to investigate some mechanisms of internal dissipation. In particular, we want to focus our attention on dissipation in materials (as concrete) which presents voids typically characterized by a coin shape, and materials (as enriched concrete e.g. Scerrato et al. 2014;2016) containing microscopic components such as micro-fillers used to improve damping performance without compromising mechanical strength. Indeed, it is found that the energy dissipation of the concrete increases with the increasing content of micro particles. On the other hand, the increasing percentage of micro-particles addition can aggravate the mechanical strength of the material. Thus, there is a reasonable compromise in incorporating these micro-particles to obtain higher damping without weakening the mechanical properties. To model such a mechanism, a microstructural independent kinematical variable φ is introduced to take into account the interaction between opposite faces of the voids whenever they came into contact because of an external load. We assume that the deformation energy of the considered medium is characterized by a volume density, Ψ, which depends on the kinematic descriptors, namely the usual displacement field $\boldsymbol{u}$ and the new scalar field φ

$$\Psi(E,\varphi) = \frac{1}{2}(2\,\mu\, E\cdot E + \lambda\,(\mathrm{tr}E)^2) + \frac{1}{2}\kappa(\varphi) + \alpha(\varphi, I_2^d) \qquad (1)$$

where λ and μ are Lamé's parameters for linearly elastic isotropic materials and E is the second order small strain tensor. The function κ is a monotonic function of the micro-sliding φ which takes into account the energy required to deform elastically the micro-cracks and α is a coupling energy term which depends upon the scalar quantity I_2^d, i.e. the second invariant of the deviatoric strain tensor. In particular, we assume for these two functions the following form

$$\kappa(\varphi) = \frac{1}{2}K_1\varphi^2 + \frac{1}{3}K_2\varphi^3 + \frac{1}{4}K_3\varphi^4$$

$$\alpha\left(\varphi, I_2^d\right) = -K_\alpha\varphi\sqrt{I_2^d}$$

where K_1, K_2, K_3 and K_α are material parameters.
In order to model the dissipation, assumed to be a Coulomb-type friction, a Rayleigh potential R, is introduced as follows

$$R = \mathrm{tr}E\,\frac{\zeta}{\eta}(\log(\cosh(\eta\,\dot{\varphi}\,)))$$

where æ and ç are constitutive constants. The derivative of R with respect to the velocity $\dot{\varphi}$ can, therefore, be considered as a dissipative volume force, namely

$$F = \zeta\,\mathrm{tr}E\,(\tanh(\eta\,\dot{\varphi}\,))$$

The constitutive energy assumption presented above has been applied to three-dimensional samples under cyclic loading to show the behavior of the proposed model evaluating dissipative loops. The simulations obtained show a good agreement with measured loops.

References

Scerrato, D., Giorgio, I., Madeo, A., Limam, A. and Darve, F., 2014. A simple non-linear model for internal friction in modified concrete. *International Journal of Engineering Science*, 80, pp. 136–152.

Scerrato, D., Giorgio, I., Della Corte, A., Madeo, A., Dowling, N. E. and Darve, F., 2016. Towards the design of an enriched concrete with enhanced dissipation performances. *Cement and Concrete Research*, 84, pp. 48–61.

Scerrato, D., Giorgio, I., Della Corte, A., Madeo, A. and Limam, A., 2015 A micro-structural model for dissipation phenomena in the concrete. *Int. J. Numer. Anal. Meth. Geomech.*, 39(18), pp. 2037–2052.

Mesoscale numerical investigation of aggregate size effect in concrete through the discrete element method

Z. Ran*, **S. Y. Alam*** **& A. Loukili***

**Institut de Recherche en Génie Civil et Mécanique (GeM), UMR-CNRS 6183, Ecole Centrale de Nantes, France*

ran.zhu@ec-nantes.fr, syed-yasir.alam@ec-nantes.fr, ahmed.loukili@ec-nantes.fr

Abstract. The fracture behavior of concrete has been modelled by the discrete element method (DEM). A new contact model has been adopted in this study. For micro parameters determination, the Levenberg-Marquardt (LM) algorithm has been used. The results show that the DEM approach can be suitable for modeling the local fracture behavior of concrete.

1. Introduction

Concrete is a typical quasi-brittle material. Compared with other materials, its mechanical behavior and rupture processes are indeed complicated. The microstructure features of concrete such as aggregate size, shape and volume fraction have certain effects on its macroscopic mechanisms, as they lead to the development of a microcracking zone which causes large energy dissipation. Macroscopic mechanical models explicitly take into account the nonlinear zone where the microcracking occurs. The local fracture characteristics cannot be captured. So the numerical investigation of concrete behavior at the meso-scale has been carried out by the Discrete Element Modeling (DEM).

2. DEM approach

The particle elements are assumed to be rigid discs in 2D. These particles can overlap or detach, when the system is subjected to mechanical actions. The concept of DEM is based on the translational and rotational movements of particles due to forces and moments which act at the contact point between the particles. The micro-parameters of the insert contact bond model in DEM could not satisfy the compressive strength and tensile strength, simultaneously. The reason is that the tensile strength and compressive strength are increased with the increase of the bond tensile strength ($\overline{\sigma}_c$). However, for brittle materials like rock and concrete, the compressive strength is about one order of magnitude larger than the tensile strength. As a result, the micro parameter $\overline{\sigma}_c$ for the compressive strength is about one order of magnitude larger than the one for the tensile strength. So in this paper, the model developed by Ding and Zhang (2014) has been adopted. The new model introduces β_1 to control the contribution of moments to the maximum normal($\overline{\sigma}_{\max}, \overline{\sigma}_{\max} > 0$ in tension) and shear($\overline{\tau}_{\max}$) contact stresses, as expressed below:

$$\begin{cases} \overline{\sigma}_{\max} = \dfrac{\overline{F}_n}{A} + \beta_1 \dfrac{\overline{M}_s \overline{R}}{I} \\ \overline{\tau}_{\max} = \dfrac{\overline{F}_s}{A} \end{cases} \tag{7}$$

where $\overline{F}_n, \overline{F}_s, \overline{M}_n$ and $\overline{M}_s$ are the contact forces and moments at the center of the contact zone, respectively, in the normal(n) and shear(s) directions; β_1 is ranging from 0 to 1.

The new contact model also assumes that the shear strength follows the Coulomb criterion. In the new contact model, the shear strength is determined by:

$$\begin{cases} \tau_s = \sigma_n \tan\varphi + \bar{c} & if\ \sigma_n \tan\varphi < (\gamma - 1)\bar{c} \\ \tau_s = \gamma \bar{c} & if\ \sigma_n \tan\varphi \geq (\gamma - 1)\bar{c} \end{cases} \quad (8)$$

where σ_n is the average normal stress, and $\sigma_n = \bar{F}_n / \bar{A}$; $\bar{c}$ is the cohesion strength; φ is the friction angle and γ is the parameter that determines the ratio of the maximum shear strength over the cohesion strength.

After shear failure, the cohesion is set to zero and the frictional angle can decrease to residual angle φ_r and the shear strength is determined by:

$$\tau_s = \sigma_n \tan\varphi_r \quad (9)$$

2.1 Development and calibration of parameters for mortar

The numerical model with a size of 40×40mm was generated for an unconfined compression test and the model with a size of 110×400mm for a direct tension test. In addition, the comparison between the experimental results and the modeling results are listed in Table 1.

Table 1. Comparison between laboratory tests and modeling results

Mechanical properties	Experiment Results	DEM Modeling
Elastic modulus E (GPa)	24.0	23.6
Poisson's ratio ν	0.30	0.33
Compressive strength σ_c (MPa)	50.0	50.0
Tensile Strength σ_t (MPa)	1.9-2.1	2.05

Table 1 demonstrates that the new contact model can satisfy both the compression test and the direct tension test with the same parameters at the same time.

3. Concrete Modeling

The size of the specimen for modeling is 0.11×0.22m^2 for a compression test and Φ=0.11m for a Brazilian test in 2D for concrete with different aggregate sizes. Aggregates are modeled by using clusters. A cluster is defined as a set of particles that are bonded to one another (**Erreur ! Source du renvoi introuvable.**); intra-cluster particles in clustered material have rotational velocities.

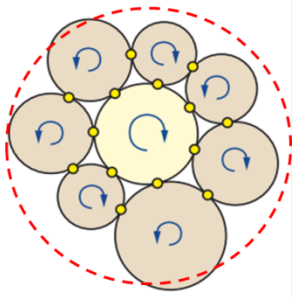

Figure 1. Cluster particles

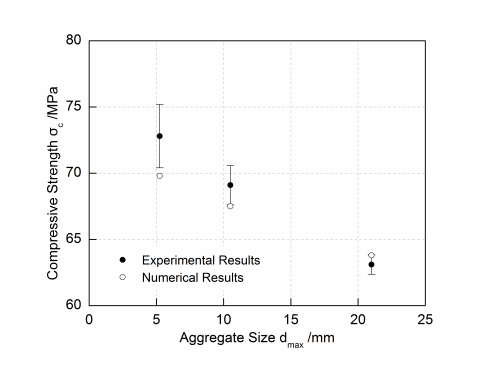

a) Compressive Strength

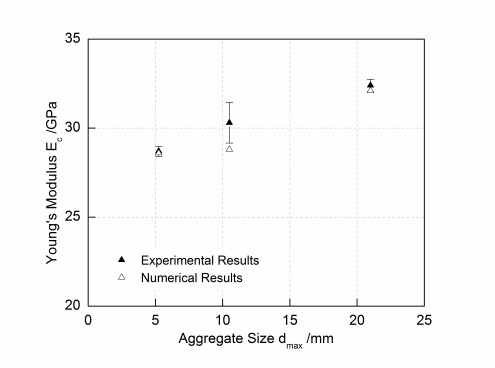

b) Young's Modulus

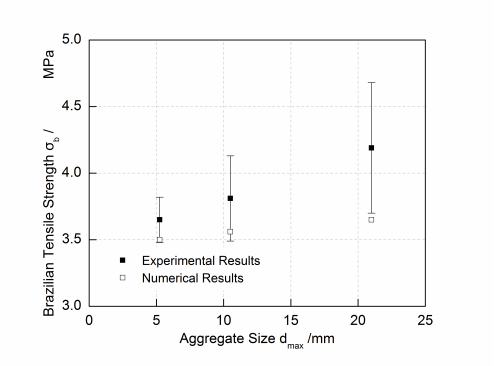

c) Brazilian Tensile Strength

Figure 2. Comparison numerical and experimental results

Erreur ! Source du renvoi introuvable. illustrates that the modeling results can properly predict then behavior of concrete both in compression and tension.

4. Conclusion

The DEM modeling approach can be used in concrete fracture modeling by modifying the default model insert in DEM.
Cluster particles can properly model the fact that aggregates can break in the tests.
DEM is suitable for investigating the local fracture behavior in the fracture processes of concrete.

Reference

Ding, X. and L. Zhang, 2014. A new contact model to improve the simulated ratio of unconfined compressive strength to tensile strength in bonded particle models. *International journal of rock mechanics and mining sciences* 69, pp.111-119.

Introducing practical constitutive soil modelling tools for teaching-learning-training purposes

Zhen-Yu Yin*

**Research Institute of Civil Engineering and Mechanics (GeM), UMR CNRS 6183, Ecole Centrale de Nantes, Nantes 44321, France*
zhenyu.yin@gmail.com

Constitutive models play an important role in the design and construction of geotechnical engineering. To date, there are hundreds of different soil constitutive models, varying from micro to macro. However, most engineers are still unable to fully understand constitutive models and have invariably chosen a model based on their own limited experiences, hoping that a "one-size-fits-all" approach can solve all engineering problems. Also they struggle with writing a computer program that can implement the soil model to achieve such a simulation. To address this problem, it would be highly useful to develop a tool that can model soil tests by choosing from a variety of constitutive models.

Today, an impressive variety of constitutive models have been developed for soils in geotechnical engineering. More parameters to be determined are generally required before the model can be applied to solving engineering problems; this poses a considerable challenge for engineers. Therefore, an efficient procedure, in conjunction with a tool for parameter identification, should be developed.

A modelling tool (ErosLab) for soil laboratory tests is presented here. First, the different kinds of tests that can be used with the tool are briefly introduced. Second, its general framework, including its mixed language programming and six main features, is presented. Third, its graphical user interface and usage instructions are illustrated. Finally, the development of an optimisation-based parameter identification tool (ErosOpt) for geotechnical engineering is described with case studies. The developed softwares can be freely downloaded from the following URL: http://www.geoinvention.com/en/news.asp?big=14.

Since the development of constitutive models with parameters identification is usually based on laboratory tests, developing these tools should be first helpful for research purposes of constitutive modelling. Even though field-scale problems cannot be directly simulated, the debugging scheme in this tool includes complex loading combinations reflecting various in-situ conditions. Furthermore, these tools can be used for teaching purposes to present the basic constitutive modelling of soil behaviours with parameters identification, especially for postgraduate students specializing in civil engineering, water conservancy, transportation, railways, and engineering geology. It can also be used for relevant professional scientific research purposes.

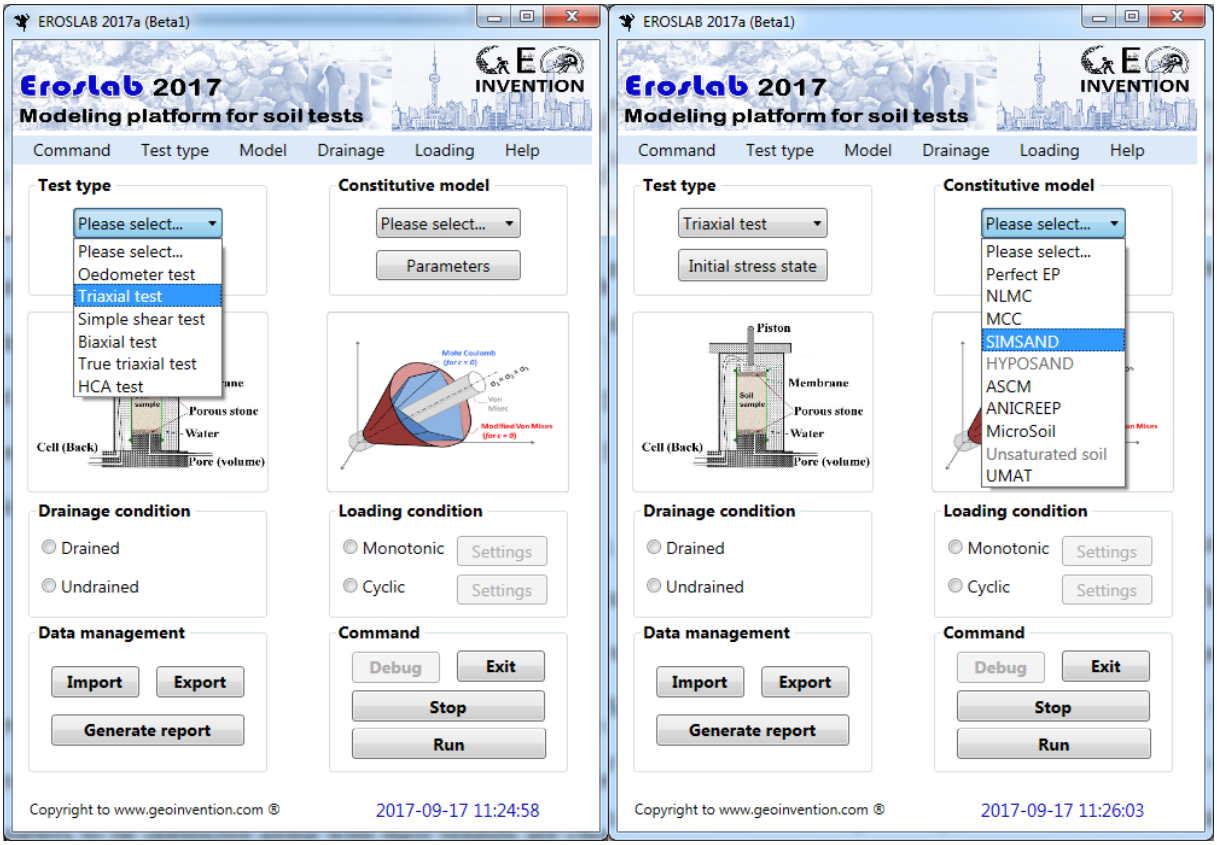

(a) **(b)**

Fig. 1. GUI window for the list of (a) test types and initial stress state, and (b) constitutive models

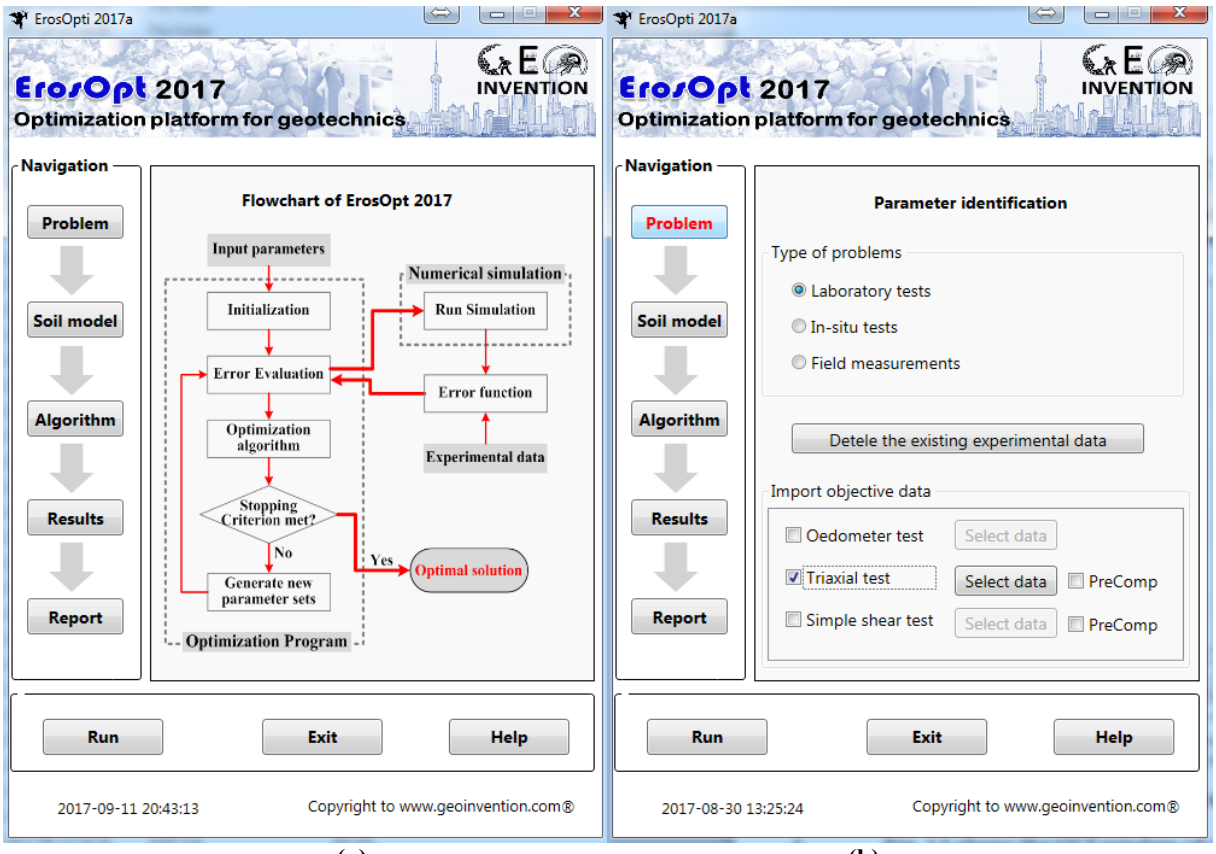

(a) **(b)**

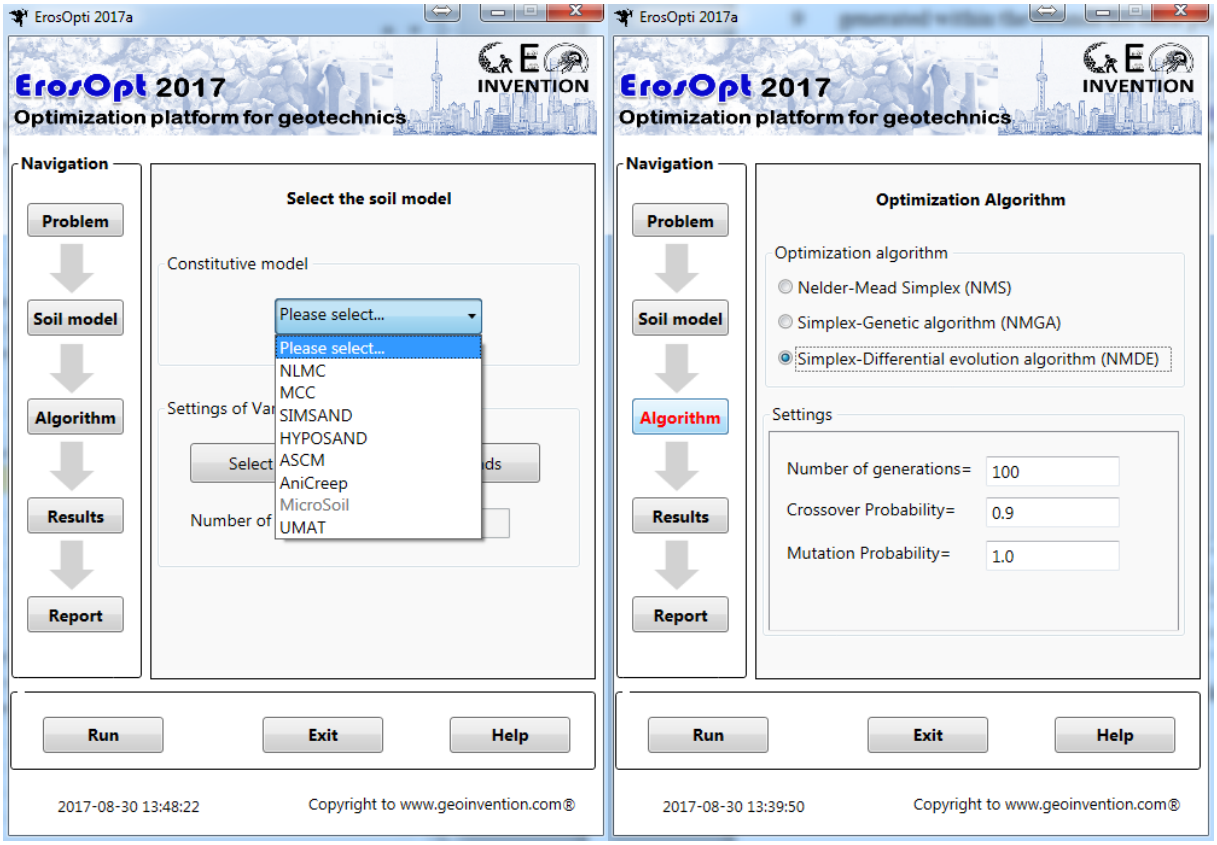

(c) **(d)**

Fig. 2. Main GUI window for (a) start page in ErosOpt, (b) for selecting problem and importing the objective data, (c) for selecting soil models, and (d) for selecting optimization algorithm

References

Jin, Y.-F., Yin, Z.-Y., Shen, S.-L., Hicher, P.-Y.: Selection of sand models and identification of parameters using an enhanced genetic algorithm. *Int. J. Numer. Anal. Methods Geomech.* 40(8), 1219-1240 (2016). doi:10.1002/nag.2487

Yin, Z.-Y., Jin, Y.-F., Shen, J.S., Hicher, P.-Y.: Optimization techniques for identifying soil parameters in geotechnical engineering: Comparative study and enhancement. *Int. J. Numer. Anal. Methods Geomech.* , n/a-n/a (2017). doi:10.1002/nag.2714

Yin, Z. Y., Xu, Q. and Hicher, P. Y., 2013. A simple critical state based double-yield-surface model for clay behavior under complex loading. *Acta Geotechnica*, 8(5), pp. 509-523.

Yin, Z.Y., Karstunen, M., Chang, C.S., Koskinen, M., Lojander, M.: Modeling Time-Dependent Behavior of Soft Sensitive Clay. *Journal of Geotechnical and Geoenvironmental Engineering* 137(11), 1103-1113 (2011). doi:10.1061/(asce)gt.1943-5606.0000527

Double-scale modelling of the hydro-mechanical behaviour of a clay rock including the effect of the microstructure

B. Pardoen *, P. Bésuelle *, J. Desrues * & S. Dal Pont *

**Univ. Grenoble Alpes, CNRS, Grenoble INP [ǂ], 3SR, 38000 Grenoble, France*
[ǂ] Institute of Engineering Univ. Grenoble Alpes
pierre.besuelle@3sr-grenoble.fr

An approach for modelling the hydro-mechanical coupled behaviour of Callovo-Oxfordian claystone (COx), a potential host rock for deep repositories of radioactive waste in France is investigated. The approach presented is a double-scale finite element method (FEM^2) using elementary areas (EA) to model the material behaviour at the microscale. The homogenised response of the microscale EA serves as implicit numerical constitutive law for the macroscale at each integration point (Figure 1). The microscale hydro-mechanical model is based on deformable grains linked by damageable cohesive interfaces. The interstitial fluid can flow through the interfaces whose hydraulic conductivity depends on their opening (Frey *et al*., 2013, van den Eijden *et al*., 2016).
At the macroscale, the field equilibrium equations have been defined for a poro-mechanical continuum, including a regularisation method for second gradient continuum (Collin *et al.*, 2006). The latter has introduced an internal length that restores mesh objectivity in the presence of strain localisation.

The work focuses on the definition of the EA in a clay rock, in order to be both a realistic and simple representation of the material. Experimental observations and characterisations of the rock's microstructure are considered to define the material in a realistic manner (Robinet *et al.*, 2012,). The microstructure is described by the different grain mineralogies, the size and shape of grains of each mineralogy (mean grain size, elongation, preferential orientation, etc…) and their distribution (Figure 2).

The influence of the microstructure is investigated on the macro response. Numerical simulations of plane strain compression tests allows the effect on strain localisation and fluid flow through the specimen to be studied.

The variability of the microscopic behaviour has been highlighted by considering a microstructural-based variability in terms of mineral phase repartition. At larger or intermediate scales, the representativeness of the natural heterogeneity and variability of clay rock can be improved through the spatial variability of the EAs at the Gauss points of the macro-FE-model.

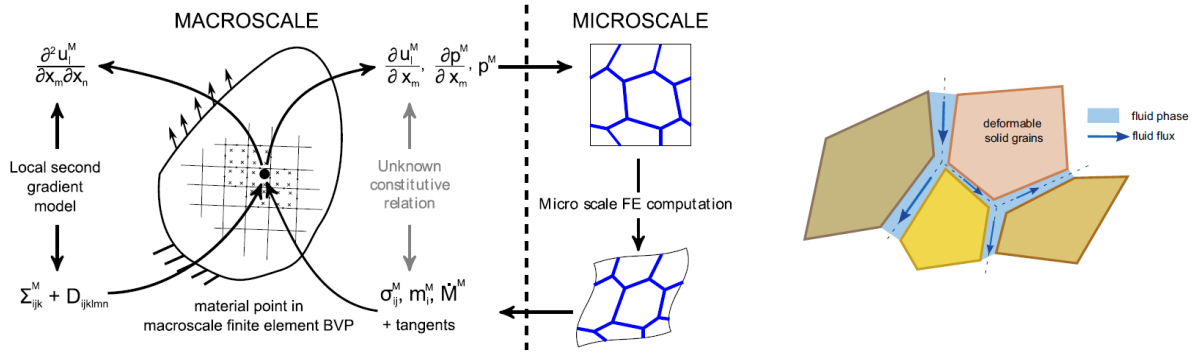

Figure 1. (left) Schematic representation of the FE^2 method for hydromechanical coupling with a local second gradient paradigm and (right) concept of the micromechanical model (van den Eijnden *et al.*, 2017)

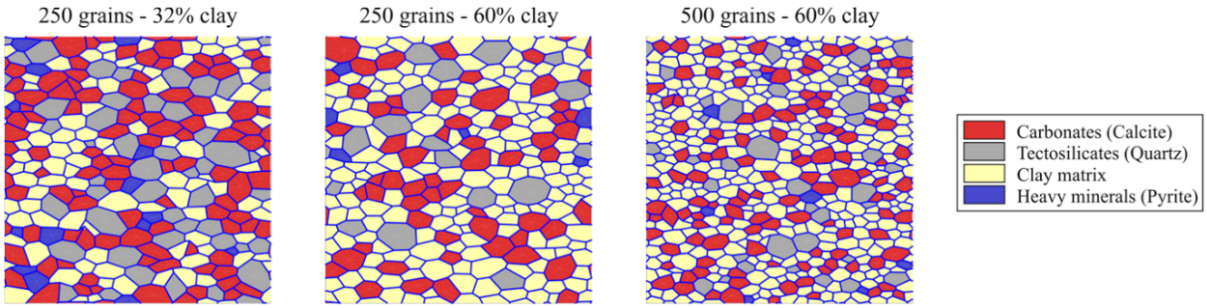

Figure 2. Examples of realistic microstructures with different clay contents and grain numbers

References

Collin, F., Chambon, R., Charlier, R., 2006. A finite element method for poro mechanical modelling of geotechnical problems using local second gradient models. *Int. J. Numer. Meth. Engng*. 65(11), pp. 1749–1772.

Fauchille, A.L., 2015. Déterminismes microstructuraux et minéralogiques de la fissuration hydrique dans les argilites de Tournemire : apports couplés de la pétrographie quantitative et de la corrélation d'images numériques. *Ph.D. thesis*, Université de Poitiers, Poitiers.

Frey, J., Chambon, R., Dascalu, C., 2013. A two-scale poromechanical model for cohesive rocks. *Acta Geotech*. 8(2), pp. 107–124.

Robinet, J.C., Sardini, P., Coelho, D., Parneix, J.C., Prêt, D., Sammartino, S., Boller, E., Altmann, S., 2012. Effects of mineral distribution at mesoscopic scale on solute diffusion in a clay-rich rock: Example of the Callovo-oxfordian mudstone (Bure, France). *Water Resour. Res.,* 48, W05554.

van den Eijnden, A., Bésuelle, P., Chambon, R., Collin, F., 2016. A FE^2 modelling approach to hydromechanical coupling in cracking-induced localization problems. *Int. J. Solids Struct.,* 97-98, pp. 475–488.

van den Eijnden, A., Bésuelle, P., Collin, F., Chambon, R., Desrues, J., 2017. Modeling the strain localization around an underground gallery with a hydro-mechanical double scale model; effect of anisotropy. *Comput. Geotech*., 85, pp. 384–400.